pubs.acs.org/Biomac

Article

Liposomes Decorated with 2-(4′-Aminophenyl)benzothiazole Effectively Inhibit $A\beta_{1-42}$ Fibril Formation and Exhibit in Vitro Brain-Targeting Potential

Spyridon Mourtas,* Barbara Mavroidi, Antonia Marazioti, Maria Kannavou, Marina Sagnou, Maria Pelecanou, and Sophia G. Antimisiaris

Cite This: https://dx.doi.org/10.1021/acs.biomac.0c00811

Read Online

ACCESS | Metrics & More | Article Recommendations | Supporting Information

ABSTRACT: The potential of 2-benzothiazolyl-decorated liposomes as theragnostic systems for Alzheimer's disease was evaluated in vitro, using PEGylated liposomes that were decorated with two types of 2-benzothiazoles: (i) the unsubstituted 2-benzothiazole (BTH) and (ii) the 2-(4-aminophenyl)benzothiazole (AP-BTH). The lipid derivatives of both BTH-lipid and AP-BTH-lipid were synthesized, for insertion in liposome membranes. Liposomes (LIP) containing three different concentrations of benzothiazoles (5, 10, and 20%) were formulated, and their stability, integrity in the presence of serum proteins, and their ability to inhibit β-amyloid (1−42) (Aβ42) peptide aggregation (by circular dichroism (CD) and thioflavin T (ThT) assay), were evaluated. Additionally, the interaction of some LIP with an in vitro model of the blood−brain barrier (BBB) was studied. All liposome types ranged between 92 and 105 nm, with the exception of the 20% AP-BTH-LIP that were larger (180 nm). The 5 and 10% AP-BTH-LIP were stable when stored at 4 °C for 40 days and demonstrated high integrity in the presence of serum proteins for 7 days at 37 °C. Interestingly, CD experiments revealed that the AP-BTH-LIP substantially interacted with Aβ42 peptides and inhibited fibril formation, as verified by ThT assay, in contrast with the BTH-LIP, which had no effect. The 5 and 10% AP-BTH-LIP were the most effective in inhibiting Aβ42 fibril formation. Surprisingly, the AP-BTH-LIP, especially the 5% ones, demonstrated high interaction with brain endothelial cells and high capability to be transported across the BBB model. Taken together, the current results reveal that the 5% AP-BTH-LIP are of high interest as novel targeted theragnostic systems against AD, justifying further in vitro and in vivo exploitation.

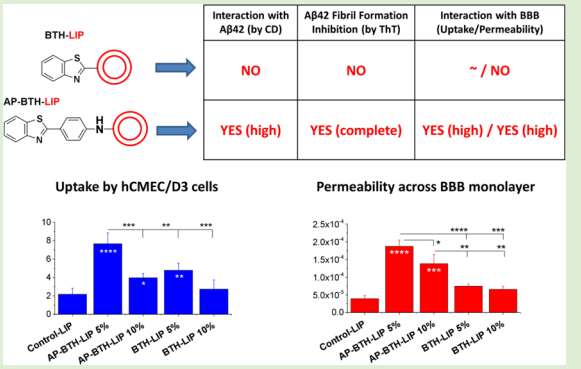

1. INTRODUCTION

Alzheimer's disease (AD) is a disorder of the central nervous system (CNS) that progressively leads to the degeneration of neurons. Although the exact causes of AD are still not fully understood, the amyloid and tau hypotheses currently dominate AD research efforts. The amyloid hypothesis is related to the aggregation of β-amyloid peptides (Aβ), which leads to their accumulation in the brain and to the formation of extracellular amyloid plaques, leading to inflammation.[1−3] At the molecular level, the unbalanced production and clearance of Aβ results in increased levels of Aβ monomers in the brain, leading to the formation of larger soluble oligomers that form aggregates, and finally, insoluble amyloid fibrils, which are the main constituents of the amyloid plaques. Several reports suggest that Aβ soluble oligomers are responsible for synaptic dysfunction and cognitive impairment (which are associated with AD).[4−8]

In this context, strategies aiming at targeting the production, aggregation, and clearance of Aβ species for theragnostic purposes are currently being exploited. One such strategy is the development of functionalized nanoparticles (NP) to efficiently target the blood−brain barrier (BBB) and also the amyloid species.[9,10] Indeed, the surface functionalization of NPs has been extensively applied as a method to enhance the accumulation of NP-encapsulated drugs at specific body sites due to the increased binding affinity of the NPs to specific receptors as a result of multivalent effects.[11,12] Between the various NP types, liposomes are usually preferred as drug carriers because they are structurally versatile and also highly biocompatible. Moreover, liposome PEGylation, which refers to the coating of the vesicle surface with polyethylene glycol molecules, can efficiently reduce the rapid clearance of

Received: May 26, 2020
Revised: October 13, 2020

liposomes by macrophages and prolong their circulation time in the blood.[13,14]

In several previous investigations, curcumin and various curcumin derivatives were demonstrated to (i) effectively inhibit the formation of Aβ oligomers, (ii) to rescue cells from Aβ-induced toxicity (at micromolar concentrations in vitro)[15−20] and (iii) to reduce the brain concentrations of amyloids in vivo.[21,22] Curcuminoid-decorated liposomes demonstrated high affinity (K_D: 1−5 nM) for Aβ42 fibrils,[23] similar to the affinity (K_D: 0.5−2 nM) of liposomes that were functionalized with a monoclonal antibody against Aβ.[24] Phosphatidic acid (PA) and cardiolipin (CL)[25] are two other substances that were used for the surface modification of liposomes. However, they exhibited only moderate binding affinity for aggregated forms of Aβ42 (K_D: 22−60 nM). Finally, liposomes decorated with tetracycline derivatives have also been considered as systems for AD diagnosis/therapy.[26]

The benzothiazole heterocycle is a versatile scaffold in medicinal chemistry, possessing a wide spectrum of activities.[27,28] In addition to their well-documented anticancer properties, benzothiazole and its derivatives are well associated with the search for therapeutics (or diagnostics) for Alzheimer's disease (AD). Unsubstituted 2-benzothiazole compounds as well as substituted or more complicated compounds[29−32] have been found to effectively interact with Aβ42 species, in vitro and in vivo, and to inhibit or delay the aggregation of Aβ42 monomers.[33−36] In particular, the clinical testing of 2-(4-aminophenyl)benzothiazole derivatives showed promising results.[37−39]

In more detail, in the diagnostic area, many radiolabeled 2-phenylbenzothiazole derivatives are continuously explored as amyloid imaging agents, while an 18F-labeled derivative of phenylbenzothiazole ([18F] flutemetamol, Vizamyl, GE Healthcare) gained approval in 2013 for clinical use as a positron emission tomography (PET) diagnostic agent for AD.[40] In the therapeutic area of AD, the only available drugs are cholinesterase inhibitors (donepezil, tacrine, rivastigmine, and galantamine) that alleviate the symptoms of dementia but do not treat the disease.[41] Benzothiazoles represent a class of heterocyclic compounds which serve as a scaffold for the design of anti-amyloid agents against Alzheimer's disease.[42] More specifically, benzothiazole derivatives and complexes[27,43,44] have been demonstrated to inhibit Aβ aggregation and reduce the concentrations of soluble amyloid oligomers. Furthermore, others have tried to develop substances that combine a benzothiazole derivative with a cholinesterase inhibitor (tacrine, in most cases) with the aim to achieve concomitant enhancement of cholinergic neurotransmission and reduction of Aβ aggregation.[45−49]

However, with the exception of the benzothiazole metal complex,[44] the issue of crossing the BBB has not been addressed, despite the fact that it remains the major issue in the failure of AD drug development.[50] In fact, benzothiazole derivatives were never considered up-to-date for the construction of potential therapeutic nanosystems, via conjugation/immobilization on the surface of NPs. The only benzothiazolyl-decorated NP that is reported describes the development of unsubstituted 2-benzothiazole liposomes,[51] but their interaction with amyloid species and their potential to be transported across the BBB were not evaluated.

Herein, taking into consideration the capability of benzothiazoles to interact with Aβ42 and the known potential of nanotechnologies to enhance the function of active compounds that are immobilized on their surface due to multivalency, we study for the first time, the activity of benzothiazolyl liposomes toward Aβ species. In more detail, we compare two different types of benzothiazolyl liposomes for their potential to interact with Aβ42 and inhibit Aβ42 aggregation: (i) unsubstituted 2-benzothiazole (BTH)-decorated liposomes (BTH-LIP), which were formed as previously reported,[51] and (ii) 2-arylsubstituted benzothiazole (AP-BTH)-decorated liposomes (AP-BTH-LIP), which were formed after establishing an appropriate methodology for the synthesis of stable vesicles.

The interactions of BTH-LIP and AP-BTH-LIP with Aβ42 species and their inhibitory effect on Aβ42 aggregation were studied by circular dichroism (CD) spectropolarimetry[52] and by means of the thioflavin T (ThT) assay.[53] Both LIP types were additionally evaluated for their potential to be transported across the blood−brain barrier (BBB) in an in vitro cellular model,[54−56] to evaluate whether or not additional ligands (homing devices) should be attached to consider them as nanotherapeutic modalities for AD.

2. EXPERIMENTAL SECTION

All chemicals required for the synthesis of the lipid derivatives were obtained from Sigma-Aldrich (Darmstadt, Germany). Silica-gel-60 F254 TLC plates were obtained from Merck (Darmstadt, Germany). TLC visualization methods included UV light, charring with aqueous solution of potassium permanganate ($KMnO_4$) (freshly prepared), ninhydrin, or molybdenum blue spray, all purchased from Sigma-Aldrich (Darmstadt, Germany). Flash column chromatography for the purification of the organic synthesis products was carried out on silica gel (230−400 mesh) from Merck (Darmstadt, Germany). A Shimadzu LC-2010 liquid chromatography HPLC system (Canby, OR, USA) was used for sample analysis. Samples were eluted through an RP18 (5 μm particle size) LiChroCART 250-4 column. A Brucker DPX 400 MHz NMR instrument (Peoria, IL, USA) was used, and the sample spectra were recorded at 25 °C. Chemical shifts were referenced to the corresponding solvent peaks and are reported in ppm.

1,2-Distearoyl-*sn*-glycerol-3-phosphatidylcholine (DSPC) and 1,2-distearoyl-*sn*-glycerol-3-phosphoethanolamine-*N*-[methoxy-(polyethyleneglycol)-2000] (PEG) were obtained from Avanti Polar Lipids (Alabaster, AL, USA). Fluorescein-isothiocyanate-dextran-4000 (FITC), calcein, cholesterol (Chol), lucifer yellow-CH dilithium salt (LY), Triton X-100, Sephadex G-50, and Sepharose CL-4B were purchased from Sigma-Aldrich (Darmstadt, DE). Fetal calf serum (FCS) was obtained from Invitrogen. For measurements of protein concentrations, Bradford microassay was applied (Biorad, Hercules, CA, USA). Any other chemicals used were purchased from Sigma-Aldrich or Merck.

For the liposome preparation, a bath sonicator (Branson, Thermo Fisher Scientific, Waltham, MA, USA) or a microtip-probe high-intensity sonicator (Sonics and Materials, Leics, UK) was used. For their purification, size exclusion chromatography was performed on Sepharose CL-4B (Sigma-Aldrich, Darmstadt, Germany). A Shimatzu RF-1501 spectrofluorometer (Shimatzu, Kyoto, JP) was used for the measurement of the fluorescence intensity (FI) of calcein or FITC in samples (EX/EM 490 nm/525 nm; 5 nm slits).

2.1. Synthesis of BTH and AP-BTH Lipid Derivatives.

2.1.1. Synthesis of BTH-Lipid (3). Palmitic acid (532 mg, 0.78 mmol) dissolved in DCM (7.5 mL) was placed in a round-bottomed flask, and the solution was cooled at 4 °C. Diisopropylcarbodiimide (DIC) (133 μL, 0.85 mmol, 1,1 equiv), which was used as an activation agent, was added, and the palmitic acid was activated for 15 min at 4 °C. 2-Aminophenyl disulfide dissolved in DCM (500 μL) was added to the activated palmitic acid, and the reaction mixture was stirred overnight at room temperature. It was then directly acidified using an aqueous solution of citric acid (15% w/v, 5 mL), and the organic layer was washed with H_2O (3 × 5 mL) and further dried and evaporated. The oily residue was further dissolved in a mixture of THF/MeOH (6 mL,

https://dx.doi.org/10.1021/acs.biomac.0c00811
Biomacromolecules XXXX, XXX, XXX−XXX

Table 1. Liposome Types, Lipid Membrane Composition (in Mole Ratios), and Physicochemical Properties[a]

liposome type	DSPC/Chol/PEG/LIPID[b] molar ratio	mean hydrodynamic diameter (nm)	polydispersity index (PDI)	ζ-potential (mV)
Control	1:1:0.15	80.2 ± 5.1	0.154	−1.32 ± 0.17
BTH-LIP (5%)	1:1:0.15:0.05	97.2 ± 3.5	0.206	−2.67 ± 0.15
BTH-LIP (10%)	1:1:0.15:0.10	99.4 ± 4.5	0.230	−3.21 ± 0.71
BTH-LIP (20%)	1:1:0.15:0.20	104.5 ± 3.7	0.218	−2.79 ± 0.20
AP-BTH-LIP (5%)	1:1:0.15:0.05	92.5 ± 5.2	0.143	−2.51 ± 0.35
AP-BTH-LIP (10%)	1:1:0.15:0.10	102.5 ± 7.6	0.229	−2.02 ± 0.18
AP-BTH-LIP (20%)	1:1:0.15:0.20	180.2 ± 5.1	0.234	−1.54 ± 0.02

[a]The values reported are mean values from five measurements of three independent samples. The percent values used for the BTH-LIP and AP-BTH-LIP naming is based on the content of BTH-lipid and AP-BTH-lipid (5%, 10 or 20%) in the vesicles expressed as percent of the DSPC content. [b]LIPID is AP-BTH-lipid or BTH-lipid.

5:1), and the solution was flushed with gaseous N_2. To this, $NaBH_4$ (34 mg, 0.90 mmol) was added, and the reaction mixture was stirred for 3 h at room temperature and then acidified with AcOH (515 μL, 9.0 mmol) followed by further stirring for 1 h (under an N_2 atmosphere). Finally, the solvents were evaporated under reduced pressure, and the oily residue was crystallized using anhydrous EtOH and AcCN. Total yield: 55%. The final product showed a single spot in TLC analysis and was further analyzed by HPLC and ^{1}H NMR. The HPLC chromatogram and the assignments of ^{1}H NMR spectrum are shown in the Supporting Information (Figures S1A and S2A). ^{1}H NMR ($CDCl_3$) δ ppm: 0.88 (6H, t), 1.26 (58H, s), 1.59 (4H, m), 2.26 & 2.29 (4H, 2 t), 3.01 (2H, t), 3.47 (2H, t), 4.13−4.36 (4H, 4dd), 5.26 (1H, m), 7.39 (1H, t), 7.48 (1H, t), 7.84 (1H, d), 8.00 (1H, d).

2.1.2. Synthesis of Lipid-2-(4-aminophenyl)benzothiazole (AP-BTH-Lipid) (6). 2.1.2.1. Synthesis of 2-(4′-Aminophenyl)-benzothiazole (AP-BTH) (4). 2-Aminobenzenethiol (1.25 g, 10 mmol) and 4-aminobenzoic acid (1.37 g, 10 mmol) were mixed in a round-bottomed flask, and polyphosphoric acid (20 g) was added. The reaction mixture was heated at 220 °C for 4 h, and the reaction mixture was slowly poured into ice-cold aqueous Na_2CO_3 (10% w/v). The precipitated product was filtered and washed with H_2O, and finally, it was recrystallized from a mixture of MeOH/H_2O to afford 2-(4′-aminophenyl)benzothiazole as a light brown powder (yield: 64%). The isolated product was verified by ^{1}H NMR analysis. The HPLC chromatogram and the assignments of the ^{1}H NMR spectrum are shown in the Supporting Information (Figure S2B). ^{1}H NMR (MeOD) δ ppm: 6.75 (2H, d), 7.33 (1H, t), 7.45 (1H, t), 7.80 (2H, d), 7.89 (2H, m).

2.1.2.2. Synthesis of N-[4-(Benzothiazol-2-yl)-phenyl]-succinamic Acid [Also Named 3-(4-(Benzothiazol-2-yl)phenylcarbamoyl)-propanoic Acid] (5). 2-(4′-Aminophenyl)benzothiazole (**4**) (99.3 mg, 0.44 mmol) and succinic anhydride (43.91 mg, 0.44 mmol) were placed in a round-bottomed flask and dissolved in $CHCl_3$ (approx. 2 mL), and the reaction mixture was stirred overnight at room temperature. Next, the solvent was almost completely evaporated, and Et_2O was added. The solid that was formed was filtered, washed with Et_2O, and finally dried (yield: 90%). The isolated product was verified by ^{1}H NMR analysis. The HPLC chromatogram and the assignments of the ^{1}H NMR spectrum are shown in the Supporting Information (Figure S2C). ^{1}H NMR (MeOD) δ ppm: 2.70 (4H, 2 t), 7.42 (1H, t), 7.52 (1H, t), 7.76 (2H, d), 7.99 (2H, d), 8.04 (2H, d).

2.1.2.3. Synthesis of AP-BTH-Lipid (6). *N*-[4-(Benzothiazol-2-yl)-phenyl]-succinamic acid (21.4 mg, 0.0656 mmol) and *N*-hydroxysuccinimide (NHS) (7.92 mg, 0.0688 mmol) were diluted in DMF/DCM (300 μL, 1:1), and the mixture was added in a round-bottomed flask. For carboxylic acid activation, diisopropylcarbodiimide (DIC) (0.0688 mmol, 10.7 μL) was added, and the mixture was stirred for 5 min at room temperature. DSPE-PEG_{2000}-NH_2 (60 mg, 0.0219 mmol) was added, and the reaction mixture was stirred overnight. Next, the mixture was diluted with DCM (10 mL), and the organic phase was washed with H_2O (3 × 10 mL) and brine (3 × 5 mL) and then separated and further dried and evaporated. The remaining oil was purified using EtOAc/Hex at 65 °C and finally dried (yield: 55%). The isolated DSPE-PEG_{2000}-AP-BTH product (AP-BTH-lipid) showed a single spot in TLC analysis (by UV light and by charring with a freshly prepared aqueous solution of potassium permanganate and molybdenum blue reagent) and was further analyzed by HPLC and ^{1}H NMR. The HPLC chromatogram and the assignments of the ^{1}H NMR spectrum are shown in the Supporting Information (Figures S1B and S2D). ^{1}H NMR (MeOD) δ ppm: 0.90 (6H, t), 1.28 (56H, m), 1.60 (4H, m), 2.30 & 2.33 (4H, 2 t), 2.60 (2H, t), 2.73 (2H, t), 3.34−3.62 (∼180H, m), 3.90 (2H, d), 3.99 (2H, t), 4.16−4.19 (2H, t & 1H, d), 4.42 (1H, 1d), 5.22 (1H, m), 7.42 (1H, t), 7.52 (1H, t), 7.78 (2H, d), 7.99 (d, 2H), 8.05 (d, 2H).

2.2. Preparation of Liposomes. Small unilamellar vesicle (SUV) liposomes, having the lipid compositions reported in Table 1, were prepared by the thin film hydration method and high-intensity sonication, as reported in detail previously.[51,55,56] Liposomes were usually dispersed in phosphate-buffered saline (10 mM; pH 7.40; 300 mOsm). When FITC (36 mM) of calcein (100 mM) was encapsulated in the liposomes, the osmotic pressure of the solutions was adjusted to be isotonic. After formation, the liposome dispersions were annealed to heal any structural defects at 60 °C for 1 h. Liposome purification from nonentrapped materials was carried out, if needed, by size-exclusion chromatography on a Sepharose 4B-CL or Sephadex G-50 (medium) column (40 × 1 cm) that was eluted with PBS pH 7.40. The Stewart assay was used for the measurement of the phospholipid concentration of liposomes.[57]

2.3. Liposome Properties. *2.3.1. Physicochemical Properties and Physical Stability.* The mean hydrodynamic diameter and the polydispersity index (PDI) of the vesicles (dispersed in PBS at 0.2 mg/mL phospholipid concentration) was measured by dynamic light scattering (DLS) at 25 °C (173° angle) on a Malvern Nano-ZS (Malvern Instruments, Worcestershire, UK). Zeta potential (ζ-potential) values were measured also at 25 °C in the same samples by Doppler electrophoresis.

The vesicle physical stability was studied by measuring the mean diameter, PDI, and ζ-potential, periodically during storage (4 °C, 40 days).

2.3.2. Liposome Integrity in the Presence of Serum Proteins. To monitor the integrity of AP-BTH-LIP and control liposomes (control-LIP), calcein-encapsulating liposomes (1 mg/mL phospholipid) were incubated at 37 °C in PBS as well as in FCS (80% v/v). As mentioned above, calcein was encapsulated in the liposomes at 100 mM concentration, where quenching of fluorescence is realized. Calcein latency (%) and retention (%) values were calculated at various time points, by taking samples from the incubated materials and measuring calcein FI, as described in detail previously.[51,55,56]

2.4. Inhibition of Aβ1−42 (Aβ42) Peptide Fibril Formation by Liposomes. *2.4.1. Preparation of Aβ and Liposome Samples.* The amyloid Aβ42 peptide (Anaspec, USA, >95% pure) was gradually dissolved with gentle tapping (without vortexing) in Type 1 H_2O (Milli-Q) to 100 μM. The solutions of plain Aβ42 in phosphate buffer (PB, 10 mM, pH 7.33) were then prepared by gradual dilutions until a final concentration of 50 μM. In the preparation of the Aβ/liposome mixtures, the ratios of 1:0.75, 1:0.50, 1:0.25, and 1:0.10 were calculated based on the amount of Lipid-BTH or Lipid-AP-BTH incorporated to liposomes (Section 2.2). Based on the lipid membrane composition (in mole ratios), the proper volumes (μL) of liposome stock solutions were added in Aβ solutions to achieve a final concentration of 37.5, 25, 12.5,

https://dx.doi.org/10.1021/acs.biomac.0c00811
Biomacromolecules XXXX, XXX, XXX−XXX

Scheme 1. Synthesis of BTH-Lipid

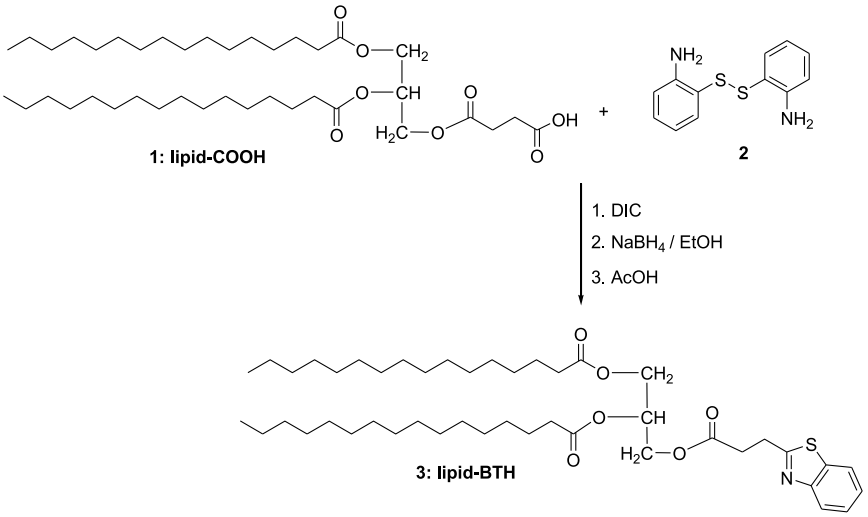

and 5 μM Lipid-BTH or Lipid-AP-BTH. The solutions of plain Aβ42 and control liposomes (without BTH-lipid or AP-BTH-lipid) at the same concentrations and incubation conditions were used as control experiments for comparison.

2.4.2. Circular Dichroism (CD) Studies. Aβ structural changes were monitored under quiescent conditions for 15 days at 33 °C. The CD spectra were recorded in the range of 190−260 nm on a JASCO J-715 spectropolarimeter (Jasco Co., Japan). Each spectrum is the average from three scans (rate 100 nm·min^{-1}, resolution 0.5 nm). Three independent experiments were performed for each condition and for solutions of plain Aβ. Control liposomes (without BTH-lipid or AP-BTH-lipid) were also studied. The CD data were analyzed using the OriginPro 9 program.

2.4.3. Thioflavin T (ThT) Assay. For the ThT (Sigma-Aldrich, USA; >97% pure) assay, the 15 day-aged CD solutions of Aβ42 (with or without liposomes) were diluted with PBS (10 mM, pH 7.33) to obtain theoretical Aβ42 concentration of 25 μM, and ThT in PBS (10 mM, pH 7.33) was added (5 μM). The mixture was well agitated, and the FIe was monitored with a HITACHI F-2500 spectrofluorometer at an excitation of 440 nm (emission slit = 2.5 nm, PMT voltage 700 V, response 0.4 s). The analysis of the FIe data was performed using the OriginPro 9 program.

2.5. Cell Studies. HEK cells (Human HEK-293 embryonic kidney cells, American Type Culture Collection, VA) were cultured in RPMI 1640 medium (supplemented with 1% antibiotic−antimycotic solution and 10% FBS (Invitrogen, Carlsbad, CA, USA)) at 37 °C, 5% CO_2/saturated humidity.

hCMEC/D3 cells (immortalized human cerebral microvascular endothelial cells that were obtained under license from the Institut National de la Sante et de la RechercheMedicale (INSERM, Paris, FR), at passage 25−35) were cultured in EndoGro medium (Merck, Darmstadt, DE), as described in detail previously.[55,56]

U-87 MG cells (human glioblastoma−astrocytoma cells, acquired from the cell bank of the Laboratory of Radiobiology, Institute of Nuclear & Radiological Sciences and Technology, Energy & Safety, NCSR "Demokritos" (Athens, Greece)) were cultured in Dulbecco's modified Eagle's medium (DMEM), supplemented with 10% FBS, penicillin, glutamine, and streptomycin. Cell cultures were maintained in flasks and grown at 37 °C in a humidified atmosphere of 5% CO_2 in air.

2.5.1. Cytotoxicity Assay. The cytotoxicity of LIP toward HEK and hCMEC/D3 was evaluated by incubating LIP (7 nmol) with cells (3×10^4) for 4 h (37 °C, 5% CO_2/saturated humidity). A 48 h incubation was also performed, in some cases, to evaluate the potential cytotoxicity of AP-BTH-LIP types. In all cases, the MTT assay was used as described in detail previously.[55,56]

A cell cytotoxicity assay in U-87MG glioblastoma cells was also conducted to investigate the effect of AP-BTH-LIP and BTH-LIP on the Aβ-induced cell toxicity. In brief, U-87 MG cells (~8000 cells/well) were incubated with Aβ solutions (1 μM) in the presence of liposomes (Aβ: liposome ratios of 1:0.5 and 1:1) for 24 h at 37 °C. MTT assay was also used for this study.

2.5.2. Cell Uptake. The uptake of liposomes by cells was studied with FITC-entrapping LIP after incubation with hCMEC/D3 cells (200 nmol liposomal lipid/10^6 cells) for 4 h at 37 °C. After washing the cells (twice with ice-cold PBS), they were detached using scrappers and suspended in PBS. After cell lysis with Triton X-100 (2% v/v, final concentration), the FI was measured (EX-490 nm/EM-525 nm, slits 5 nm). Any autofluorescence of the empty cells was subtracted. The protein content of the cell samples was measured by Bradford assay. Finally, the calculated FITC uptake values (%) were normalized for their protein concentration.

To exclude the possibility of the uptake of free dye (that may have leaked out from LIP), free FITC was also incubated with the cells under identical conditions, and it was proved that no free FITC was taken up by the cells.

2.5.3. Cell-Monolayer Permeation Studies. For monolayer preparation studies, the cells were seeded on Transwell filters (polycarbonate six-well, pore size 0.4 μm; Millipore Merck, Darmstadt, DE) precoated with type I collagen, at 5×10^4 cells/cm^2. The detailed procedure followed, and the tests carried out to verify that the monolayer produced is intact (transendothelial electrical resistance measurements (TEER) and Lucifer yellow (LY) permeability calculation) are described in detail elsewhere.[55,56]

For liposome transport evaluation, FITC-containing liposomes were placed on the monolayers (200 nmol per monolayer) in medium containing 10% (v/v) FCS at 37 °C for 60 min. At selected time points, the transport of FITC was calculated after measuring FITC-FI at 490−520 nm, in the receptor compartment of the transwell systems. LY was also used to verify that vesicles do not modify the properties of the barrier. Control liposomes were also evaluated for comparison.

2.6. Transmission Electron Microscopy (TEM). The vesicular morphology of the liposomal preparations was recorded by means of TEM. Two types of AP-BTH-LIP (5 and 10%) were resuspended (1 mg/mL) in 10 mM HEPES and then stained with 1% neutral phosphotungstic acid (PTA) (dissolved in dH_2O), washed two times with dH_2O, drained with tissue paper, and observed with a JEOL (JEM-2100) TEM (Jeol, Tokyo, JP) at 100.000 eV.[58]

TEM studies were also conducted with the Aβ42 peptide incubated in the presence of 5% AP-BTH-LIP (ratio 1:1, 50 μM) for 15 days at 33 °C under quiescent conditions. As controls, Aβ42 plain peptides (a) and 5% AP-BTH-LIP (b), incubated under identical conditions, were also studied. The samples were stained with PTA, as mentioned above.

https://dx.doi.org/10.1021/acs.biomac.0c00811
Biomacromolecules XXXX, XXX, XXX−XXX

Scheme 2. Synthesis of Lipid-2-(4-aminophenyl)benzothiazole (AP-BTH-lipid)

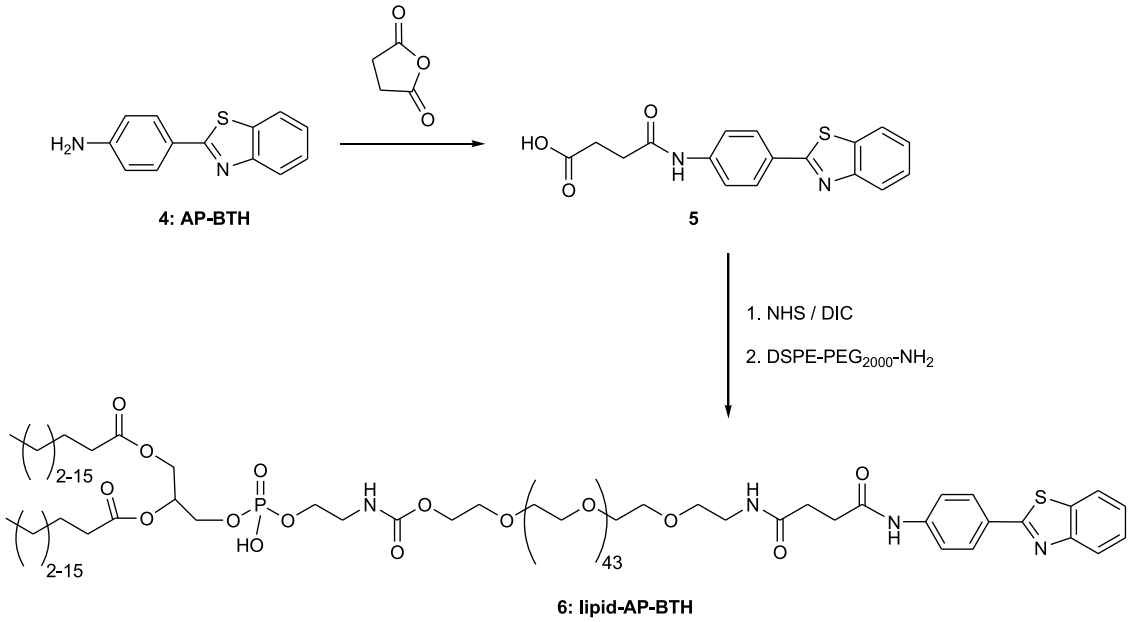

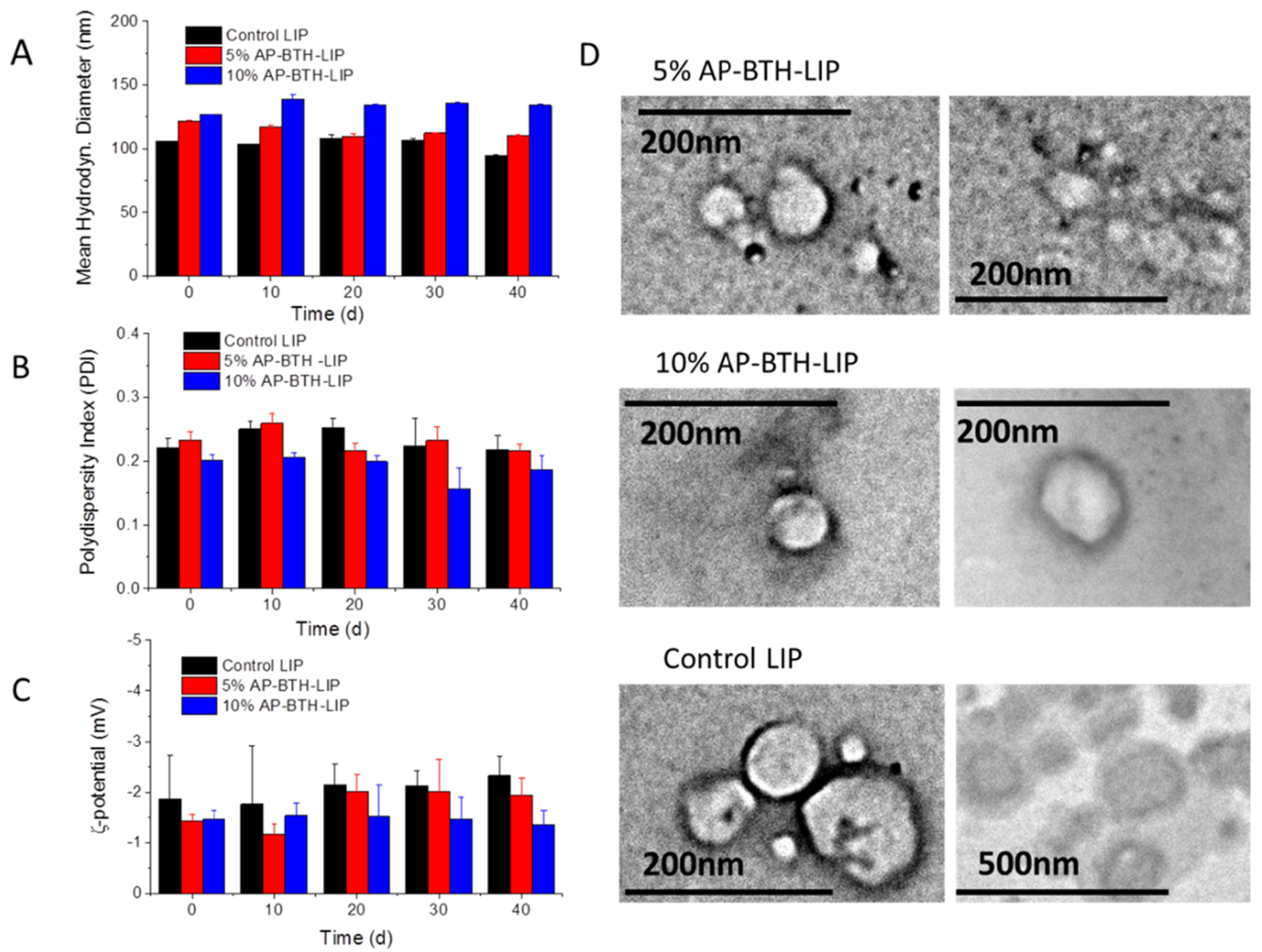

Figure 1. (A) Mean diameter values, (B) PDI values, and (C) and zeta potential values of 5% AP-BTH-LIP, 10% AP-BTH-LIP, and control-LIP during storage at 4 °C, for up to 40 days. Liposomal dispersion in PBS buffer (lipid concentration 5 mg/mL). Each value is the mean of five measurements (bars represent SD values of each mean). (D) TEM micrographs of the 5% AP-BTH-LIP and 10% AP-BTH-LIP.

https://dx.doi.org/10.1021/acs.biomac.0c00811
Biomacromolecules XXXX, XXX, XXX−XXX

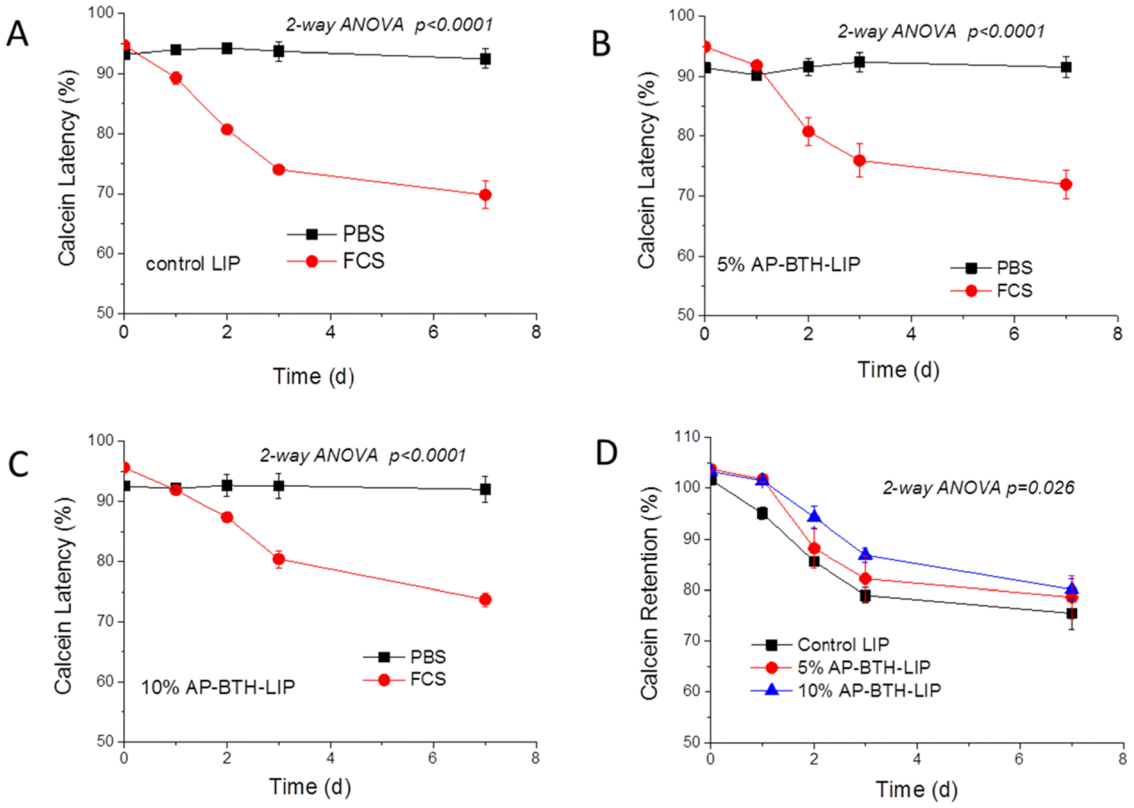

Figure 2. Calcein latency (%) in (A) control-LIP, (B) 5% AP-BTH-LIP, and (C) 10% AP-BTH-LIP during incubation in PBS buffer and FCS for 7 days at 37 °C. (D) Calcein retention (%) in the same liposome types during incubation in FCS. Liposomes were incubated at 1 mg/mL lipid concentration.

2.7. Statistical Analysis. The results are reported as mean ± SD (from three or four independent experiments). One-way ANOVA followed by the Bonferroni post hoc test was applied for the calculation of statistical significance (at $p = 0.05$). Two-way ANOVA was performed when more factors were compared. The significance of all comparisons made is presented in the figures.

3. RESULTS

3.1. Synthesis of BTH-Lipid (3). BTH-lipid was synthesized as already described by our group.[51] In brief, lipid-COOH (**1**) was activated with diisopropylcarbodiimide (DIC) and reacted with 2-aminophenyl disulfide and then treated with sodium borohydride ($NaBH_4$) to achieve reduction and thiol liberation. To this, acetic acid (AcOH) was added to favor the ring closure[51] and the formation of the BTH-lipid (**3**) (Scheme 1).

3.2. Synthesis of Lipid-2-(4-aminophenyl)-benzothiazole (AP-BTH-Lipid) (6). For the synthesis of lipid-2-(4-aminophenyl)benzothiazole (AP-BTH-lipid) (**6**), the 2-(4′-aminophenyl)benzothiazole derivative (AP-BTH) (**4**) was first synthesized,[59] and this was further reacted with succinic anhydride to the corresponding *N*-[4-(benzothiazol-2-yl)-phenyl]-succinamic acid (**5**). In the last step of the synthesis, **5** was conjugated with DSPE-PEG_{2000}-NH_2, in the presence of *N*-hydroxysuccinimide (NHS)/DIC, to obtain the desired AP-BTH-lipid (**6**) (Scheme 2).

3.3. Preparation of Liposomes (LIP). Small unilamellar vesicles (SUVs) with the lipid compositions reported in Table 1 were prepared.[51,55,56]

3.4. Physicochemical Properties of AP-BTH-LIP. The molecular composition and properties of the various liposomal formulations are reported in Table 1. In addition to AP-BTH-LIP, with various concentrations of AP-BTH-lipid in their membranes, BTH-LIP and control-LIP (without AP-BTH or BTH group) were also studied for comparison. DSPC and Chol were used to have rigid-membrane liposomes. PEG was used for the prolongation of blood circulation of vesicles to improve their potential to be distributed in tissues; indeed vesicles with increased physical stability and strong interbilayer repulsion provided by the PEGylated outer surface of the vesicles can overcome attractive forces and be more stable (compared to non-PEGylated vesicles) after in vivo administration.[60,61] It should be noted that the only difference between the control-LIP and the BTH/AP-BTH-LIP is the presence of the BTH/AP-BTH groups on the decorated ones, while all liposome formulations (control and the decorated ones) have a DSPE-PEG-OMe lipid, to introduce the PEG protecting group, at the same percentage. The exact lipid and molar compositions of our nanoliposomes are presented in Table 1.

3.4.1. Physicochemical Properties of AP-BTH-LIP. The mean hydrodynamic diameter of the various AP-BTH-LIP was approximately 100 nm or less (Table 1), and it was found to be at a similar range for the AP-BTH-LIP as well, with the exception of the 20% AP-BTH-LIP that had a significantly increased mean diameter (180 nm). Polydispersity values were always below 0.234, indicating that a highly uniform sample with respect to the particle size was formed.[62] The zeta potential values were always close to zero, as anticipated due to the fact that the vesicles were PEGylated, the lipids used were zwitterionic, and the measurements were carried out in high salt content.[63]

https://dx.doi.org/10.1021/acs.biomac.0c00811
Biomacromolecules XXXX, XXX, XXX−XXX

The physical stability of 5 and 10% AP-BTH-LIP was studied by monitoring their size distribution and ζ-potential, during storage for 40 days at 5 °C. Control-LIP (without any lipid conjugate) were also monitored. In Figure 1A−C, it is seen that both the mean diameter and the PDI values remained unchanged during the 40 days period. More specifically, mean diameters ranged between 110 and 120 nm for 5% AP-BTH-LIP and between 130 and 140 nm for the 10% AP-BTH-LIP, while PDI values did not exceed 0.25 for all vesicles. The ζ-potential values were also found to be stable during the 40 days storage period, with values starting from −1.42 ± 0.14 for the 5% AP-BTH-LIP and − 1.47 ± 0.16 for the 10% AP-BTH-LIP.

Moreover, these novel 5 and 10% AP-BTH-LIP exhibited a round vesicular morphology as it was recorded by means of TEM (Figure 1D), which also revealed the size of the vesicles and confirmed those measured by DLS (Table 1).

3.4.2. Integrity of AP-BTH-LIP during Incubation in Serum Proteins (Calcein Studies). Both 5 and 10% AP-BTH-LIP (as well as control liposomes) were studied for their integrity during their incubation in buffer and FCS for a 7 day time period at 37 °C. The results are reported in Figure 2. As seen from the calcein latency results, both types of liposomes were very stable when incubated in PBS even after 7 days (Figure 2B,C), as it was also shown for the control-LIP (Figure 2A). Additionally, all LIP types exhibited high integrity when incubated in serum proteins, having calcein latency values higher than 80% after 48 h of incubation. Their high integrity in serum proteins was also retained during continued incubation, since calcein latency values higher than 70% were measured even after 7 days of incubation (in FCS) for all the LIP types. This was anticipated for the control-LIP, due to their lipid composition (see above, in Section 2.4). Nevertheless, the calcein latency results of the AP-BTH-LIP types indicate that the incorporation of AP-BTH-lipid at the specific concentrations tested does not decrease the integrity of the control-LIP in the presence of serum proteins. In fact, the addition of AP-BTH-lipid in the liposome membrane seems to increase the calcein latency values of the liposomes during their incubation in serum proteins. This is better depicted in Figure 2D, where the retention of calcein in the liposomes is reported; calcein retention in liposomes is slightly but significantly ($p = 0.026$) increased as increasing amounts of AP-BTH-lipid are incorporated in their membranes.

3.5. Inhibition of Aβ42 Aggregation Efficiency. *3.5.1. CD Studies.* To assess the effect of the decorated liposomes (AP-BTH-LIP and BTH-LIP) on the aggregation course of Aβ42, we used circular dichroism (CD) during a 15 day study. The aggregation of Aβ produces characteristic CD spectra that reflect the conformational changes of the peptide from a β-sheet assembly (red line, negative maximum at 222 nm) to larger aggregates and finally to insoluble amyloid fibrils that precipitate from solution with the loss of the CD signal (Figure 3A).[52] The presence of inhibitors of aggregation causes changes in the typical CD spectral pattern over time, providing evidence of interaction.

Before the actual studies, the solutions of plain undecorated liposomes (LIP) with Aβ42 at different Aβ/LIP ratios, 1:0.10, 1:0.25, 1:0.50 and 1:0.75 ratios, were studied with CD to assess the effect of the presence of liposomes on the aggregation of Aβ42 and to define the optimum Aβ/liposome ratio for the CD studies. As shown in Figure S3 (Supporting Information) at the higher ratios of Aβ/LIP 1:0.75 and 1:0.50, the presence of the liposomes stabilized a β-sheet-like structure (maximum at 216 nm) of Aβ42 that did not aggregate further but remained

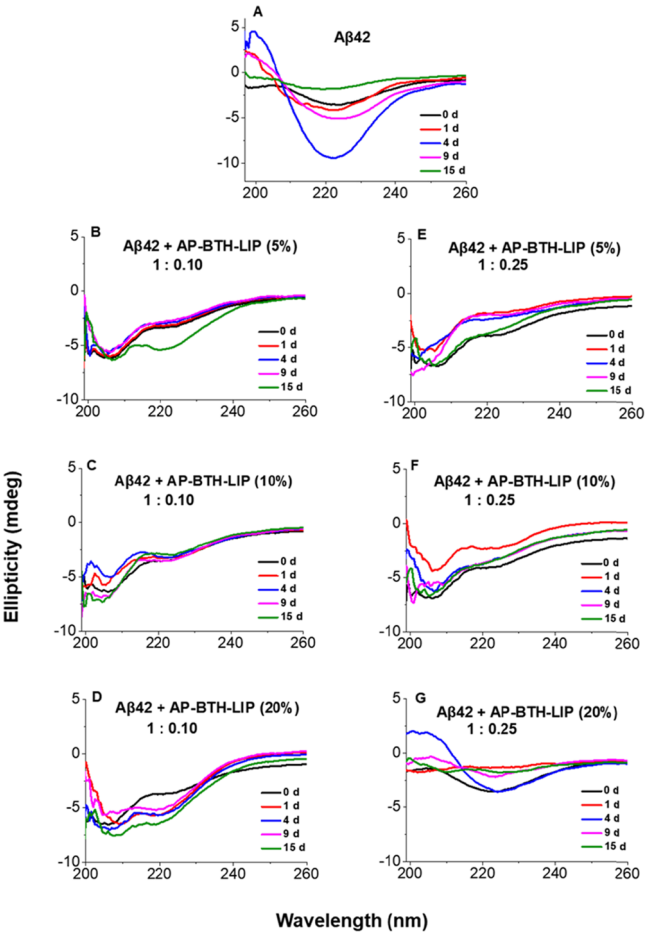

Figure 3. CD spectra of 50 μM plain solution of (A) Aβ42 as well as in the presence of (B) AP-BTH-LIP (5%), (C) AP-BTH-LIP (10%), and (D) AP-BTH-LIP (20%) at ratio 1:0.10 and in the presence of (E) AP-BTH-LIP (5%), (F) AP-BTH-LIP (10%), and (G) AP-BTH-LIP (20%) at ratio 1:0.25. Spectra were recorded for a period of 15 days at 33 °C. Representative spectra from $n = 3$ independent experiments are presented.

unaffected up to day 15, indicating an intervention of the liposome itself, in the aggregation course of Aβ42. At the lower ratios of 1:0.25 and 1:0.10, it is obvious that the interaction of the LIP with Aβ42 monomers or oligomers takes place, as observed by the presence of composite peaks (especially clear in Figure S3D, 1:0.25 ratio, negative max at 214 nm); however, the equilibrium is eventually shifted toward aggregation, resulting in the complete loss of the signal at day 15, as observed for plain Aβ42 (Figure 3A). Based on the above, the Aβ/LIP ratios of 1:0.10 and 1:0.25 were judged appropriate for the assessment of the effect of the decorated liposomes AP-BTH-LIP and BTH-LIP on Aβ42 aggregation. In addition, the CD spectra of the dispersions of plain LIP, BTH-LIP (5, 10, and 20%), and the corresponding AP-BTH-LIP dispersions in the absence of Aβ42 were obtained under the same conditions, as the ones used in the Aβ42−liposome interaction studies, to serve as controls. They all presented a weak absorption with a negative maximum at 205 nm, relatively stronger at the 20% load, which remained unchanged for the duration of the study (Figure S4, Supporting Information).

The CD spectra of Aβ42 solutions in the presence of AP-BTH-LIP (5, 10, and 20% load) at the Aβ42/LIP ratios of 1:0.10 and 1:0.25 are shown in Figure 3. At the 1:0.10 ratio, relatively

https://dx.doi.org/10.1021/acs.biomac.0c00811
Biomacromolecules XXXX, XXX, XXX−XXX

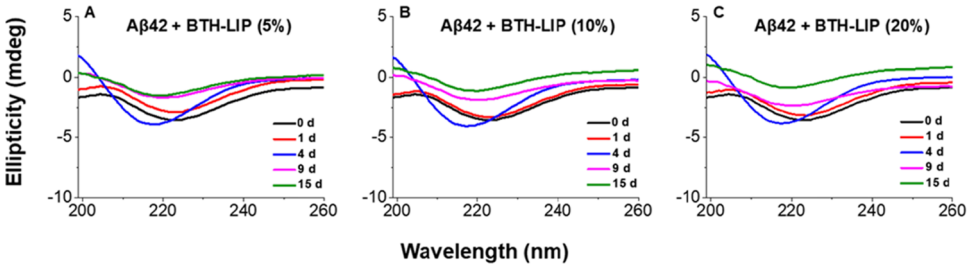

Figure 4. CD spectra of 50 μM Aβ42 solution in the presence of (A) BTH-LIP (5%), (B) BTH-LIP (10%), and (C) BTH-LIP (20%) at ratio 1:0.25. Spectra were recorded for a period of 15 days at 33 °C. Representative spectra from n = 3 independent experiments are presented.

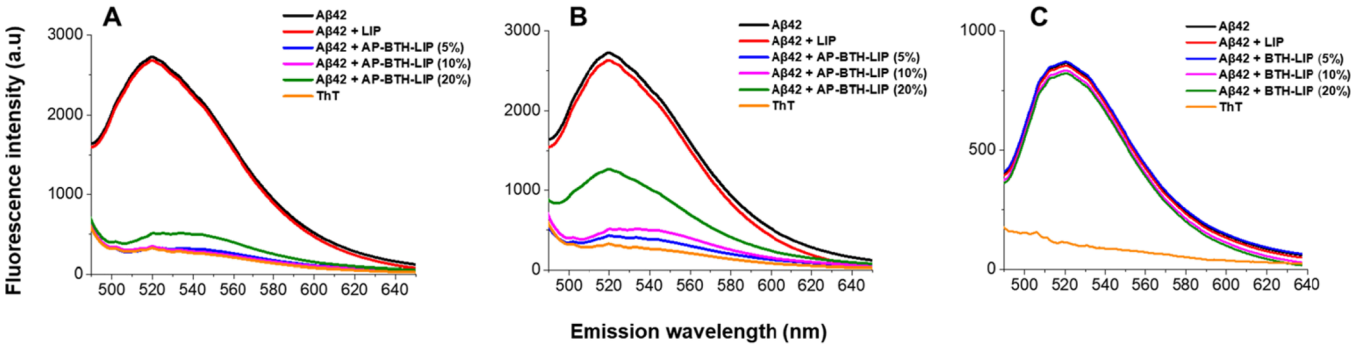

Figure 5. Fluorescence emission spectra of ThT upon binding to fibrils of Aβ42 (25 μM, 15 days) (A) in the presence of the AP-BTH-LIP at an Aβ/liposome ratio of 1:0.10, (B) in the presence of the AP-BTH-LIP at an Aβ/liposome ratio of 1:0.25, and (C) in the presence of the BTH-LIP at an Aβ/liposome ratio of 1:0.25. Fluorescence was monitored after excitation at λ = 440 nm. Representative spectra from n = 3 independent experiments are presented.

weak composite negative peaks with maxima at 205 and 222 nm are present, stronger in the case of the 20% load, attributed to AP-BTH-LIP and β-sheet assemblies, respectively, which present small changes in the duration of the study. The same holds true for the 1:0.25 ratio with the exception of the 20% load in which quick advancement of the aggregation is noted and already at day 9, the CD signal is reduced to its final value, indicating precipitation from solution. Hence, the overall, strong interaction of the AP-BTH-LIP with Aβ42 is evident, which interferes with the aggregation process. The quick precipitation noted in the presence of the reduced interaction of 20% AP-BTH-LIP with Aβ42 could be linked to the substantially larger size of these particular vesicles (compared to the other two AP-BTH-liposome types, Table 1). Another potential explanation may be that the reduced interaction is due to higher intra or intermolecular interactions of AP-BTH groups between the different liposome particles due to the hydrophobic character of AP-BTH on their surface, which may result in liposome aggregation.

The interaction of the BTH-LIP-bearing benzothiazole-lipid at 5, 10, and 20% load[51] was also studied through CD at the ratios Aβ42/BTH-LIP of 1:0.10 and 1:0.25. The CD spectra of the 1:0.10 ratio are shown in Figure 4. At both ratios, interactions are present, as evidenced by the weak spectra and the shift of the β-sheet-like negative peak to lower wavelengths (maxima at 218 nm); however, aggregation appears to precede faster compared to plain Aβ42 solutions, and the CD signal is almost at the baseline at day 15.

3.5.2. ThT Assay. The ThT dye, which is almost non-fluorescent in solution, is known to display enhanced fluorescence upon binding to typical amyloid fibrils.[64] The results of the ThT assay for both the 1:0.10 and 1:0.25 Aβ42/AP-BTH-LIP ratios are shown in Figure 5. As it can be seen in Figure 5A,B (black lines), the fluorescence intensity of the plain solutions of Aβ42 was considerably enhanced compared to the solutions of the plain ThT of the same concentration (orange lines), indicating the presence of amyloid fibrils. In the 1:0.10 ratio (Figure 5A), the presence of both 5 and 10% AP-BTH-LIP resulted in the complete inhibition of fibril formation, as observed by the lack of fluorescence intensity, while in the 20% load, a very weak fluorescence signal is present, indicating the presence of small amount of fibrils. The noted shift of the maximum of the signal to higher wavelengths may also be indicating the formation of alternative aggregated structures. At the higher ratio of 1:0.25 (Figure 5B), a great reduction in the fluorescence signal was also recorded in the presence of AP-BTH-LIP but less pronounced compared to the 1:0.10 ratio. The noted shift of the maximum of the signal to higher wavelengths in the case of the 5 and 10% AP-BTH-LIP, as well as the reduced amount of fibrils in the case of the 20% load while the CD absorbance has reached the baseline, may be indicating the formation of the aggregates of differentiated structure compared to typical amyloid fibrils, or even the presence of amorphous aggregates that precipitate from solution, but do not generate signal in the ThT assay.

The ThT assay results are in complete agreement with the CD study that shows the interaction of the AP-BTH liposomes with Aβ42. The interaction can only be ascribed to the presence of 2-(4′-aminophenyl)benzothiazole as both the plain non-decorated liposomes (LIP, red lines in Figure 5) and the liposomes bearing the unsubstituted benzothiazole (BTH-LIP, Figure 5C) fail to prevent fibril formation, as evidenced by the strong, comparable to that of plain Aβ42 solutions, fluorescence signal of their solutions in the ThT assay.

3.5.3. TEM Studies. To clarify the structure of Aβ42 peptides in the presence of 5% AP-BTH-LIP, TEM studies were

https://dx.doi.org/10.1021/acs.biomac.0c00811
Biomacromolecules XXXX, XXX, XXX−XXX

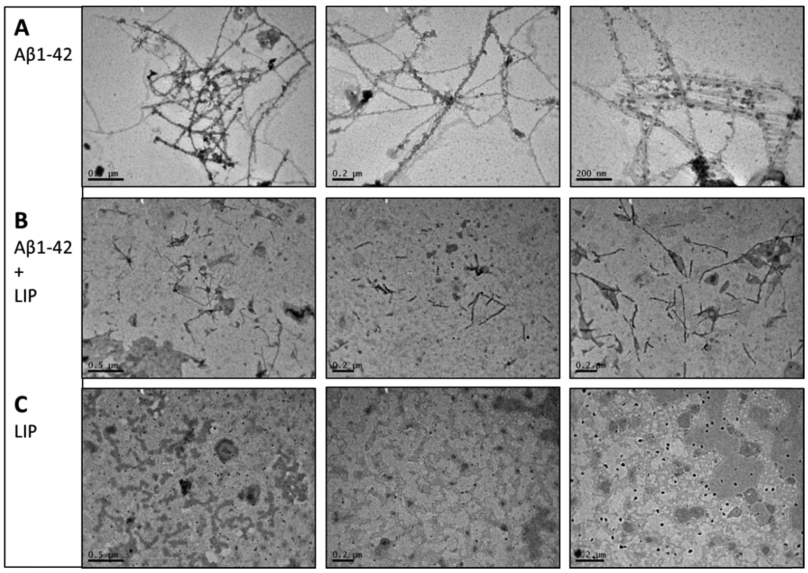

Figure 6. TEM micrographs of (A) plain Aβ42 peptides (50μM, 15 days), (B) Aβ42 peptides in the presence of 5% AP-BTH-LIP at an Aβ/liposome ratio of 1:1 (50 μM, 15 days), and (C) 5% AP-BTH-LIP (50 μM, 15 days).

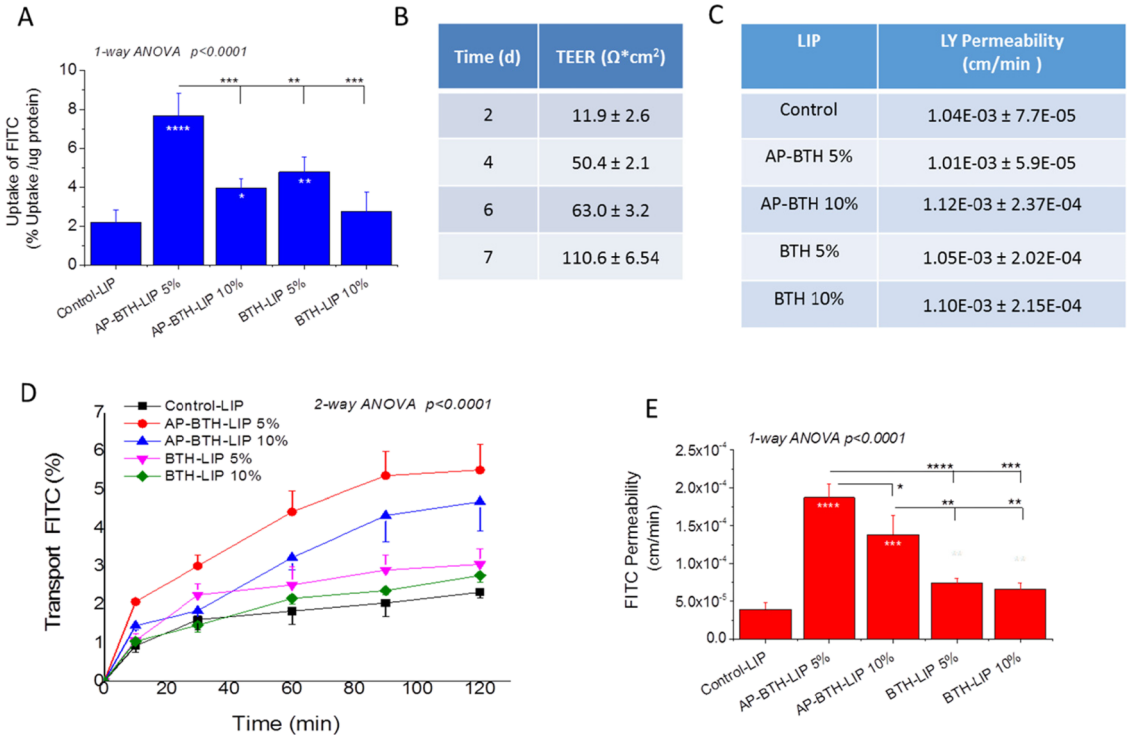

Time (d)	TEER (Ω*cm²)
2	11.9 ± 2.6
4	50.4 ± 2.1
6	63.0 ± 3.2
7	110.6 ± 6.54

LIP	LY Permeability (cm/min)
Control	1.04E-03 ± 7.7E-05
AP-BTH 5%	1.01E-03 ± 5.9E-05
AP-BTH 10%	1.12E-03 ± 2.37E-04
BTH 5%	1.05E-03 ± 2.02E-04
BTH 10%	1.10E-03 ± 2.15E-04

Figure 7. (A) Uptake of various liposome types by hCMEC/D3 cells. (B) TEER values at various time periods during the monolayer-barrier development. (C) LY permeability values in presence of the various types of liposomes tested for their permeation across the monolayers. (D) Time-frame of liposome-associated-FITC transport (%) across the in vitro BBB. (E) Permeability values of the various types of liposomes, calculated from the FITC-transport results. Each result is the mean of four independent samples. The SDs of mean values are added as bars. Asterisks show the significance of comparisons (*$P \leq 0.05$, **$P \leq 0.01$, ***$P \leq 0.001$, ****$P \leq 0.0001$). In the column graphs, the significance of difference from control-LIP is denoted as white asterisks in each column; other significant differences are shown individually.

conducted. Opposed to the typical fibril structures that are formed when plain Aβ42 peptides are used (Figure 6A), in the presence of the liposomes (Aβ42 + 5% AP-BTH-LIP), non-typical threadlike amyloid aggregate formations are present (Figure 6B). Thus, the TEM experiments are in good correlation with the CD and ThT findings.

3.6. Cell Interaction Studies. To investigate whether the insertion of AP-BTH-lipid in the liposome membrane affects their interaction with the brain−blood barrier (BBB), vesicle uptake and transport (across cell monolayers) experiments were carried out on hCMEC/D3 cells (Figure 7), which are known to have a brain endothelial phenotype and are widely used as a cellular model of the human BBB.[54]

Herein, the uptake of 5 and 10% AP-BTH-LIP and BTH-LIP, as well as control-LIP by hCMEC/D3 cells, was evaluated. It is important to mention that none of the liposomal types studied

https://dx.doi.org/10.1021/acs.biomac.0c00811
Biomacromolecules XXXX, XXX, XXX−XXX

for their interaction with hCMEC/D3 cells exhibited any cytotoxicity against the endothelial cells under the particular experimental conditions used (Figure S5, Supporting information).

As seen in Figure 7A, the level of liposomal uptake was significantly affected by the type of liposomes used ($p < 0.0001$), and more specifically by the addition of BTH or AP-BTH (and the amount [5 or 10%] added) on their surface. All the liposomes demonstrated higher uptake compared to the control-LIP, with the exception of the 10% BTH-LIP. The highest cell uptake was exhibited by the 5% AP-BTH-LIP, for which uptake values were between 1.6 and 2.8 times higher than those of the other liposome-types evaluated. Interestingly, 5% AP-BTH-LIP exhibited significantly higher uptake than the 10% AP-BTH-LIP, suggesting that perhaps the 5% amount is closer to the optimal amount of AP-BTH-lipid that should be incorporated in vesicles for optimal biological properties.

As monolayer transport experiments were also carried out, it is important to report the TEER value of the monolayer barrier as well as to confirm that the barrier was not affected by the applied vesicles. Indeed, as seen in Figure 7B, the monolayers achieved a TEER value of 110.6 ± 6.5 Ω cm^2, which is very close to the previously reported values.[55,56] Furthermore, the permeability of LY was not modulated by the presence of any of the liposomes types evaluated, as seen in Figure 7C, proving that the liposome samples do not affect the barrier function of the monolayers.

The results of the transport experiments confirmed the increased interaction of AP-BTH-LIP with the human brain cells, compared to the BTH-LIP types. In fact, similarly to the uptake study, the most effectively transported liposomal formulation across the monolayer was the 5% AP-BTH-LIP (Figure 7D), which also showed the highest permeability value (Figure 7E), compared to all the other liposome types. The permeability value calculated for 5% AP-BTH-LIP was significantly higher than that of 10% AP-BTH-LIP ($p < 0.05$) (Figure 7E). This is in good agreement with the higher uptake of the former-type liposomes by hCMEC/D3 cells, which was described earlier (Figure 7A). Both the AP-BTH-LIP evaluated had significantly higher permeability values compared with the corresponding BTH-LIP, which did not manage to exceed transport across the cellular model of the BBB, compared to the control liposomes.

Moreover, preliminary MTT cytotoxicity studies in U-87MG glioblastoma cells for 24 h provide evidence that the presence of 5% AP-BTH-LIP alleviates the Aβ-induced cell toxicity (approx. 25% at 1 μM of 5% AP-BTH-LIP, Figure S6, Supporting Information), while the 5% BTH-LIP or the control-LIP have no significant effect.

4. DISCUSSION

In continuation of our efforts to identify active nanosystems that can efficiently interfere and inhibit Aβ42 aggregation, we herein exploited for the first time the known anti-amyloid properties of 2-benzothiazole (BTH) and its 2-(4′-aminophenyl)-benzothiazole derivative (AP-BTH) in the construction of novel liposomal nanoformulations against AD. Their conjugation to lipids and incorporation into liposome lipid-membranes is considered to be an advanced method for increasing their effectiveness due to the fact that liposomes have proven potential for crossing the BBB and several liposome-based drugs are in clinical use for brain-targeted delivery. The two types of liposomes constructed bearing either BTH or AP-BTH on their surface (BTH-LIP and AP-BTH-LIP, respectively), were found to have great physicochemical stability and integrity upon incubation with serum proteins.

The results obtained through the CD studies and the ThT binding assays clearly demonstrate the strong interaction of the decorated AP-BTH-LIP with Aβ42. The results can only be ascribed to the AP-BTH moiety, as both the non-decorated liposomes (LIP) and the unsubstituted 2-benzothiazole (BTH)-decorated liposomes (BTH-LIP) did not prevent the formation of Aβ42 fibrils. The almost complete inhibition of the formation of the amyloid fibrils of Aβ42, which is a peptide with high aggregation propensity, is an important result. In addition to the reduction of amyloid fibrils, the AP-BTH-LIP may well interact with lower-order entities (oligomers, protofibrils) that are also implicated in the pathogenesis of Alzheimer's disease and, in fact, are considered to be even more important pathologic agents than amyloid fibrils.[65]

In all previous studies of benzothiazole pharmacophore derivatives and complexes presented in the Introduction section, the % of inhibition of the Aβ fibril formation, as determined by the ThT test, ranges between 16 and 72%, compared to the respective controls.[45−49] In our case, as shown in the ThT test, the novel AP-BTH-LIP prevented almost 100% the formation of fibrils at the 5 and 10% load and the 1:0.10 Aβ/AP-BTH-LIP ratio, while the inhibition results were great also at the 1:0.25 ratio. The results obtained by the biophysical studies on the Aβ fibrillation inhibitory activity of the liposomes in this study are considerably better than those mentioned above for benzothiazole derivatives, as in the case of the AP-BTH-LIP, almost 100% inhibition of fibril formation was effected. The results are also considerably better than those of other liposomic preparations incorporating bioactive compounds, such as curcumin[66,67] or a modified ApoE-derived peptide,[68] as in all these cases, a smaller % of the inhibition of Aβ42 fibril formation is reported compared to the controls. To the best of our knowledge, this is the first time that the direct interaction of the decorated liposomes with Aβ42 and the disruption of their typical aggregation course is demonstrated through CD studies, and fully confirmed by the ThT fibril binding assay. A literature search for relevant CD and ThT studies employing other types of Aβ targeting nanoformulations reveals that a relatively small number of reports exist that provide evidence of the modulation of the aggregation course of Aβ, including gold nanoparticles,[69] self-assembled curcumin-poly(carboxybetaine methacrylate) nanogels,[70] chitosan-based nanoparticles,[71] and functionalized gadolinium (Gd) nanoparticles;[72] none of the studies, however, results in the complete absence of Aβ typical fibrils, as seen in the case of the AP-BTH-LIP.

Moreover, it is highly important that the two best performing (in CD and ThT studies) types of AP-BTH-LIP (5 and 10%), and especially the 5% AP-BTH-LIP, exhibited very high capability to target and penetrate hCMEC/D3 cell membranes, although they do not have any known BBB-specific ligand on their surface. A similar BBB-targeting effect was observed previously for two other types of amyloid-targeting liposomes,[56,73] and this unexpected result was proven to implicate the RAGE transporter, which is responsible for the transport of amyloid peptides from the blood to the brain.[73] In more detail, immunoliposomes decorated with a monoclonal antibody against Aβ42 peptides (Aβ-Mab) were found to be transported across the hCMEC/D3 cellular model of the BBB by a mechanism that implicates the RAGE transporter, since the transport was substantially reduced when the monolayer was pretreated with an anti-RAGE monoclonal antibody, while the

https://dx.doi.org/10.1021/acs.biomac.0c00811
Biomacromolecules XXXX, XXX, XXX−XXX

hCMEC/D3 cells were proven to express RAGE (by western blotting). Presumably, the liposomes can bind residual Aβ peptides (which are present in the serum in which the experiments were carried out) or to Aβ peptides that are added externally, and these Aβ peptides, which are strongly bound on the surface of the liposomes, are transported by RAGE across the BBB model together with the liposome that is linked to the specific Aβ-binding compounds.[73]

Surprisingly, the permeability value calculated herein for the transport of the 5% AP-BTH-LIP across the cellular model of the BBB monolayer (Figure 7) was equal to $1.87 \times 10^{-4} \pm 1.79 \times 10^{-5}$, much higher compared to the corresponding permeability value calculated previously for liposomes with a curcumin derivative on their surface ($5.78 \times 10^{-5} \pm 0.58 \times 10^{-5}$ cm/min for TREG-LIP).[56] In fact, the permeability of the AP-BTH-LIP was similar to that reported before for dually brain-targeted liposomes and multifunctional liposomes ($1.90 \times 10^{-4} \pm 2.8 \times 10^{-5}$ cm/min and $2.51 \times 10^{-4} \pm 3.2 \times 10^{-5}$/min, respectively). Nevertheless in addition to the high affinity for amyloid peptides the high permeability of the 5% AP-BTH-LIP is probably also attributed (at least partially) to the small size of these particular vesicles (<100 nm), compared to the sizes of some of the previously studied liposome types (which ranged between 111 and 155 nm for the curcumin-derivative liposomes and the brain-targeted and multifunctional liposomes, respectively[55,56]), in accordance with previous reports about the effect of the size of vesicles on their interaction with the hCMEC/D3 BBB model.[74]

5. CONCLUSIONS

The combined effectiveness of the novel, physicochemically stable liposomes AP-BTH-LIP (5 and 10% AP-BTH-load) in inhibiting almost completely the fibrillation of Aβ42 and demonstrating a strong BBB penetration potential is unique in the field of the development of agents against AD. The remarkable multifaceted 2-(4'-aminophenyl)benzothiazole pharmacophore becomes a big asset in the formulation of the AP-BTH-LIP as it simultaneously bestows them with the two most desired properties in AD research, the anti-amyloid action and the BBB crossing capacity. Our results strongly indicate the highly advantageous nature of the 5% AP-BTH-liposomes as an ideal candidate for the Aβ-targeting therapeutic and/or diagnostic system against AD, which deserves further in vivo exploitation.

■ ASSOCIATED CONTENT

Supporting Information

The Supporting Information is available free of charge at https://pubs.acs.org/doi/10.1021/acs.biomac.0c00811.

HPLC chromatograms of the synthesized lipid derivatives; ^{1}H NMR spectra of the synthesized products; CD spectra of the plain solution of Aβ42 as well as in the presence of LIP (control); CD spectra of plain solution of LIP, AP-BTH-LIP, and BTH-LIP; cell viability of hCMEC/D3 and HEK cells in the presence of BTH/AP-BTH-LIP; effect of the BTH/AP-BTH-LIP on the cytotoxicity of Aβ42 in U-87MG glioblastoma cells (PDF)

■ AUTHOR INFORMATION

Corresponding Author

Spyridon Mourtas − *Laboratory of Pharmaceutical Technology, Dept. of Pharmacy, School of Health Sciences, University of Patras, Rio Patras 26510, Greece; Institute of Chemical Engineering Sciences, Foundation for Research and Technology Hellas (FORTH/ICES), Rio Patras 26504, Greece;* orcid.org/0000-0003-1204-1574; Phone: +30 2610-962332; Email: mourtas@upatras.gr

Authors

Barbara Mavroidi − *Institute of Biosciences & Applications, National Center for Scientific Research "Demokritos", Athens 15310, Greece*

Antonia Marazioti − *Laboratory of Pharmaceutical Technology, Dept. of Pharmacy, School of Health Sciences, University of Patras, Rio Patras 26510, Greece; Institute of Chemical Engineering Sciences, Foundation for Research and Technology Hellas (FORTH/ICES), Rio Patras 26504, Greece*

Maria Kannavou − *Laboratory of Pharmaceutical Technology, Dept. of Pharmacy, School of Health Sciences, University of Patras, Rio Patras 26510, Greece; Institute of Chemical Engineering Sciences, Foundation for Research and Technology Hellas (FORTH/ICES), Rio Patras 26504, Greece*

Marina Sagnou − *Institute of Biosciences & Applications, National Center for Scientific Research "Demokritos", Athens 15310, Greece;* orcid.org/0000-0002-4231-6658

Maria Pelecanou − *Institute of Biosciences & Applications, National Center for Scientific Research "Demokritos", Athens 15310, Greece;* orcid.org/0000-0002-7669-2424

Sophia G. Antimisiaris − *Laboratory of Pharmaceutical Technology, Dept. of Pharmacy, School of Health Sciences, University of Patras, Rio Patras 26510, Greece; Institute of Chemical Engineering Sciences, Foundation for Research and Technology Hellas (FORTH/ICES), Rio Patras 26504, Greece*

Complete contact information is available at: https://pubs.acs.org/10.1021/acs.biomac.0c00811

Author Contributions

The manuscript was written through contributions of all authors. All authors have given approval to the final version of the manuscript.

Funding

M.K., A.M., and S.G.A. acknowledge support of this work by the project "Development of Innovative Neuroprotective Neurogenerative Synthetic Micro-Neurotrophins" (MIS-5032840), which is implemented under the Special Service of the Operational Program Competitiveness Entrepreneurship and Innovation. The project is funded by the Operational Programme "Competitiveness, Entrepreneurship and Innovation" (NSRF 2014−2020) and co-financed by Greece and the European Union (European Regional Development Fund). B.M., M.S., and M.P. acknowledge support of this work by the projects "Target Identification and Development of Novel Approaches for Health and Environmental Applications" (MIS 5002514), which is implemented under the Action for the Strategic Development on the Research and Technological Sectors. The project is funded by the Operational Programme "Competitiveness, Entrepreneurship and Innovation" (NSRF 2014−2020) and co-financed by Greece and the European Union (European Regional Development Fund). B.M. gratefully acknowledges the financial support by the Stavros Niarchos Foundation (SNF) and the State Scholarships Foundation (IKY) through the implementation of the program of Industrial Fellowships at NCSR "Demokritos" and "Reinforcement of Postdoctoral Researchers − 2nd Cycle" (MIS-5033021) (European Social Fund (ESF) − Operational Programme

https://dx.doi.org/10.1021/acs.biomac.0c00811
Biomacromolecules XXXX, XXX, XXX−XXX

″Human Resources Development, Education and Lifelong Learning″), respectively.

Notes

The authors declare no competing financial interest.

■ ACKNOWLEDGMENTS

The authors are thankful to Dr. Mary Kollia and the Laboratory of Electron Microscopy and Microanalysis (L.E.M.M.), Faculty of Natural Sciences, University of Patras, for the TEM studies.

■ ABBREVIATIONS

MTT,3-(4,5-dimethylthiazol-2-yl)-2,5-diphenyltetrazolium bromide; AcCN,acetonitrile; AcOH,acetic acid; AD,Alzheimer's disease; AP-BTH,2-(4-aminophenyl)benzothiazole; BBB,blood−brain barrier; BTH,2-benzothiazole; CD,circular dichroism; $CDCl_3$,chloroform-d; $CHCl_3$,chloroform; Chol,cholesterol; CL,cardiolipin; CNS,central nervous system; CO_2,carbon dioxide; DCM,dichloromethane; dH_2O,distilled water; DIC,diisopropylcarbodiimide; DLS,dynamic light scattering; DMF,dimethylformamide; DMSO,dimethyl sulfoxide; DSPC,1,2-distearoyl-*sn*-glycerol-3-phosphatidylcholine; DSPE-PEG_{2000}-amine,1,2-distearoyl-*sn*-glycero-3-phosphoethanolamine-*N*-[amino(polyethylene glycol)-2000] (ammonium salt); Et_2O,diethyl ether; EtOAc,ethyl acetate; EtOH,ethanol; FCS,fetal calf serum; FI,fluorescence intensity; FITC,fluorescein-isothiocyanate-dextran-4000; H_2O,water; hCMEC/D3,immortalized human cerebral microvascular endothelial cells; HEK,human HEK-293 embryonic kidney cells; HEPES,(4-(2-hydroxyethyl)-1-piperazineethanesulfonic acid); Hex,hexane; HPLC,high-performance liquid chromatography; IgG,immunoglobulin G; $KMnO_4$,potassium permanganate; LIP,liposomes; LY,lucifer yellow-CH dilithium salt; MAb,monoclonal antibody; MeOD,methanol-d; MeOH,methanol; N_2,nitrogen; $NaBH_4$,sodium borohydride; NHS,*N*-Hydroxysuccinimide; NMR,nuclear magnetic resonance; NP,nanoparticles; PA,phosphatidic acid; PBS,phosphate-buffered saline; PDI,polydispersity index; PEG,1,2-distearoyl-*sn*-glycerol-3-phosphoethanolamine-*N*-[methoxy(polyethyleneglycol)-2000]; ppm,parts per million; PTA,phosphotungstic acid; RES,reticuloendothelial system; SD,standard deviation; TEER,transendothelial electrical resistance; TEM,transmission electron microscopy; THF,tetrahydrofuran; *ThT*,thioflavin T; TLC,thin-layer chromatography; UV,ultraviolet; (Aβ, Aβ1−42),β-amyloid peptide

■ REFERENCES

(1) Sanabria-Castro, A.; Alvarado-Echeverría, I.; Monge-Bonilla, C. Molecular Pathogenesis of Alzheimer's Disease: An Update. *Ann. Neurosci.* **2017**, *24*, 46−54.

(2) Kumar, K.; Kumar, A.; Keegan, R. M.; Deshmukh, R. Recent advances in the neurobiology and neuropharmacology of Alzheimer's disease. *Biomed. Pharmacother.* **2018**, *98*, 297−307.

(3) Lutz, B.; Peng, J. Deep Profiling of the Aggregated Proteome in Alzheimer's Disease: From Pathology to Disease Mechanisms. *Proteomes* **2018**, *6*, 46.

(4) Dasilva, K. A.; Shaw, J. E.; McLaurin, J. Amyloid-beta fibrillogenesis: Structural insight and therapeutic intervention. *Exp. Neurol.* **2010**, *223*, 311−321.

(5) Findeis, M. A. The role of amyloid beta peptide 42 in Alzheimer's disease. *Pharmacol. Ther.* **2007**, *116*, 266−286.

(6) De Felice, F. G.; Ferreira, S. T. Beta-amyloid production, aggregation, and clearance as targets for therapy in Alzheimer's disease. *Cell. Mol. Neurobiol.* **2002**, *22*, 545−563.

(7) Reiss, A. B.; Arain, H. A.; Stecker, M. M.; Siegart, N. M.; Kasselman, L. J. Amyloid toxicity in Alzheimer's disease. *Rev. Neurosci.* **2018**, *29*, 613−627.

(8) Takahashi, R. H.; Nagao, T.; Gouras, G. K. Plaque formation and the intraneuronal accumulation of β-amyloid in Alzheimer's disease. *Pathol. Int.* **2017**, *67*, 185−193.

(9) Saraiva, C.; Praça, C.; Ferreira, R.; Santos, T.; Ferreira, L.; Bernardino, L. Nanoparticle-mediated brain drug delivery: Overcoming blood−brain barrier to treat neurodegenerative diseases. *J Controlled Release* **2016**, *235*, 34−47.

(10) Agrawal, M.; Ajazuddina; Tripathi, D. K.; Saraf, S.; Saraf, S.; Antimisiaris, S. G.; Mourtas, S.; Hammarlund-Udenaes, M.; Alexander, A. Recent advancements in liposomes targeting strategies to cross blood-brain barrier (BBB) for the treatment of Alzheimer's disease. *J Control Release* **2017**, *260*, 61−77.

(11) Hortigüela, V.; Larrañaga, E.; Cutrale, F.; Seriola, A.; García-Díaz, M.; Lagunas, A.; Andilla, J.; Loza-Alvarez, P.; Samitier, J.; Ojosnegros, S.; Martinez, E. Nanopatterns of Surface-Bound EphrinB1 Produce Multivalent Ligand−Receptor Interactions That Tune EphB2 Receptor Clustering. *Nano Lett.* **2017**, *18*, 629−637.

(12) Li, M.-H.; Choi, S. K.; Leroueil, P. R.; Baker, J. R., Jr. Evaluating Binding Avidities of Populations of Heterogeneous Multivalent Ligand-Functionalized Nanoparticles. *ACS Nano* **2014**, *8*, 5600−5609.

(13) Bulbake, U.; Doppalapudi, S.; Kommineni, N.; Khan, W. Liposomal Formulations in Clinical Use: An Updated Review. *Pharmaceutics* **2017**, *9*, 12.

(14) Zylberberg, C.; Matosevic, S. Pharmaceutical liposomal drug delivery: a review of new delivery systems and a look at the regulatory landscape. *Drug Delivery* **2016**, *23*, 3319−3329.

(15) Ono, K.; Hasegawa, K.; Naiki, H.; Yamada, M. Curcumin has potent anti-amyloidogenic effects for Alzheimer's beta-amyloid fibrils in vitro. *J. Neurosci. Res.* **2004**, *75*, 742−750.

(16) Kim, H.; Park, B. S.; Lee, K. G.; Choi, C. Y.; Jang, S. S.; Kim, Y. H.; Lee, S. E. Effects of naturally occurring compounds on fibril formation and oxidative stress of beta-amyloid. *J. Agric. Food Chem.* **2005**, *53*, 8537−8541.

(17) Kim, D. S. H. L.; Park, S.-Y.; Kim, J.-K. Curcuminoids from curcuma longa L. (zingiberaceae) that protect PC12 rat pheochromocytoma and normal human umbilical vein endothelial cells from abeta(1-42) insult. *Neurosci. Lett.* **2001**, *303*, 57−61.

(18) Yanagisawa, D.; Taguchi, H.; Morikawa, S.; Kato, T.; Hirao, K.; Shirai, N.; Tooyama, I. Novel curcumin derivatives as potent inhibitors of amyloid β aggregation. *Biochem. Biophys. Rep.* **2015**, *4*, 357−368.

(19) Airoldi, C.; Zona, C.; Sironi, E.; Colombo, L.; Messa, M.; Aurilia, D.; Gregori, M.; Masserini, M.; Salmona, M.; Nicotra, F.; La Ferla, B. Curcumin derivatives as new ligands of Aβ peptides. *J. Biotechnol.* **2011**, *156*, 317−324.

(20) Lakey-Beitia, J.; González, Y.; Doens, D.; Stephens, D. E.; Santamaría, R.; Murillo, E.; Gutiérrez, M.; Fernández, P. L.; Rao, K. S.; Larionov, O. V.; Durant-Archibold, A. A. Assessment of Novel Curcumin Derivatives as Potent Inhibitors of Inflammation and Amyloid-β Aggregation in Alzheimer's Disease. *J. Alzheimers Dis.* **2017**, *60*, S59−S68.

(21) Yang, F.; Lim, G. P.; Begum, A. N.; Ubeda, O. J.; Simmons, M. R.; Ambegaokar, S. S.; Chen, P. P.; Kayed, R.; Glabe, C. G.; Frautschy, S. A.; Cole, G. M. Curcumin inhibits formation of amyloid beta oligomers and fibrils, binds plaques, and reduces amyloid in vivo. *J. Biol. Chem.* **2005**, *280*, 5892−5901.

(22) Okuda, M.; Fujita, Y.; Hijikuro, I.; Wada, M.; Uemura, T.; Kobayashi, Y.; Waku, T.; Tanaka, N.; Nishimoto, T.; Izumi, Y.; Kume, T.; Akaike, A.; Takahashi, T.; Sugimoto, H. A Novel Curcumin Derivative, Inhibits Amyloid-β and Tau Aggregation, and Ameliorates Cognitive Dysfunction in Senescence-Accelerated Mouse Prone 8. *J. Alzheimers Dis.* **2017**, *59*, 313−328.

(23) Mourtas, S.; Canovi, M.; Zona, C.; Aurilia, D.; Niarakis, A.; La Ferla, B.; Salmona, M.; Nicotra, F.; Gobbi, M.; Antimisiaris, S. G. Curcumin-decorated nanoliposomes with very high affinity for amyloid-β1-42 peptide. *Biomaterials* **2011**, *32*, 1635−1645.

https://dx.doi.org/10.1021/acs.biomac.0c00811
Biomacromolecules XXXX, XXX, XXX−XXX

(24) Canovi, M.; Markoutsa, E.; Lazar, A. N.; Pampalakis, G.; Clemente, C.; Re, F.; Sesana, S.; Masserini, M.; Salmona, M.; Duyckaerts, C.; Flores, O.; Gobbi, M.; Antimisiaris, S. G. The binding affinity of anti-Aβ1-42 MAb-decorated nanoliposomes to Aβ1-42 peptides in vitro and to amyloid deposits in post-mortem tissue. *Biomaterials* **2011**, *32*, 5489−5497.
(25) Gobbi, M.; Re, F.; Canovi, M.; Beeg, M.; Gregori, M.; Sesana, S.; Sonnino, S.; Brogioli, D.; Musicanti, C.; Gasco, P.; Salmona, M.; Masserini, M. E. Lipid based nanoparticles with high binding affinity for amyloid-β1-42 peptide. *Biomaterials* **2010**, *31*, 6519−6529.
(26) Airoldi, C.; Mourtas, S.; Cardona, F.; Zona, C.; Sironi, E.; D'Orazio, G.; Markoutsa, E.; Nicotra, F.; Antimisiaris, S. G.; La Ferla, B. Nanoliposomes presenting on surface a cis-glycofusedbenzopyran compound display binding affinity and aggregation inhibition ability towards Amyloid b1-42 peptide. *Eur. J. Med. Chem.* **2014**, *85*, 43−50.
(27) Keri, R. S.; Patil, M. R.; Patil, S. A.; Budagumpi, S. A comprehensive review in current developments of benzothiazole-based molecules in medicinal chemistry. *Eur. J. Med. Chem.* **2015**, *89*, 207−251.
(28) Klunk, W. E.; Wang, Y.; Huang, G. F.; Debnath, M. L.; Holt, D. P.; Mathis, C. A. Uncharged Thioflavin-T Derivatives Bind to Amyloid-Beta Protein with High Affinity and Readily Enter the Brain. *Life Sci.* **2001**, *69*, 1471−1484.
(29) Arul Murugan, N.; Zaleśny, R.; Ågren, H. Unusual binding-site-specific photophysical properties of a benzothiazole-based optical probe in amyloid beta fibrils. *Phys. Chem. Chem. Phys.* **2018**, *20*, 20334−20339.
(30) Ono, M.; Hayashi, S.; Kimura, H.; Kawashima, H.; Nakayama, M.; Saji, H. Push-pull benzothiazole derivatives as probes for detecting beta-amyloid plaques in Alzheimer's brains. *Bioorg. Med. Chem.* **2009**, *17*, 7002−7007.
(31) Okamato, M.; Gray, J. D.; Larson, C. S.; Kazom, S. F.; Soya, H.; McEwen, B. S.; Pereira, A. C. Riluzole reduces amyloid beta pathology, improves memory, and restores gene expression changes in a transgenic mouse model of early-onset Alzheimer's disease. *Transl. Psychiatry* **2018**, *8*, 153−113.
(32) Ren, S. C.; Shao, H.; Ji, W. G.; Jiang, H. H.; Xu, F.; Chen, P. Z.; Mi, Z.; Wen, B.; Zhu, G. X.; Zhu, Z. R. Riluzole prevents soluble Aβ1-42 oligomers-induced perturbation of spontaneous discharge in the hippocampal CA1 region of rats. *Amyloid* **2015**, *22*, 36−44.
(33) Song, J. M.; DiBattista, A. M.; Sung, Y. M.; Ahn, J. M.; Turner, R. S.; Yang, J.; Pak, D. T. S.; Lee, H. K.; Hoe, H. S. A tetra(ethylene glycol) derivative of benzothiazole aniline ameliorates dendritic spine density and cognitive function in a mouse model of Alzheimer's disease. *Exp. Neurol.* **2014**, *252*, 105−113.
(34) Cifelli, J. L.; Chung, T. S.; Liu, H.; Prangkio, P.; Mayer, M.; Yang, J. BenzothiazoleAmphiphiles Ameliorate Amyloid-Related Cell Toxicity and Oxidative Stress. *ACS Chem. Neurosci.* **2016**, *7*, 682−688.
(35) Jiang, L.; Zhang, M.; Tang, L.; Weng, Q.; Shen, Y.; Hua, Y.; Sheng, R. Identification of 2-subsituted benzothiazole derivatives as triple-functional agents with potential for AD therapy. *RSC Adv.* **2016**, *6*, 17318−17327.
(36) Kiritsis, C.; Mavroidi, B.; Shegani, A.; Palamaris, L.; Loudos, G.; Sagnou, M.; Pirmettis, I.; Papadopoulos, M.; Pelecanou, M. 2-(4′-Aminophenyl)benzothiazole Labeled with 99mTc-Cyclopentadienyl for Imaging β-Amyloid Plaques. *ACS Med. Chem. Lett.* **2017**, *8*, 1089−1092.
(37) Bacskai, B. J.; Frosch, M. P.; Freeman, S. H.; Raymond, S. B.; Augustinack, J. C.; Johnson, K. A.; Irizarry, M. C.; Klunk, W. E.; Mathis, C. A.; Dekosky, S. T.; Greenberg, S. M.; Hyman, B. T.; Growdon, J. H. Molecular imaging with Pittsburgh Compound B confirmed at autopsy: a case report. *Arch. Neurol.* **2007**, *64*, 431−434.
(38) Johnson, K. A.; Gregas, M.; Becker, J. A.; Kinnecom, C.; Salat, D. H.; Moran, E. K.; Smith, E. E.; Rosand, J.; Rentz, D. M.; Klunk, W. E.; Mathis, C. A.; Price, J. C.; Dekosky, S. T.; Fischman, A. J.; Greenberg, S. M. Imaging of amyloid burden and distribution in cerebral amyloid angiopathy. *Ann. Neurol.* **2007**, *62*, 229−234.
(39) Pike, K. E.; Savage, G.; Villemagne, V. L.; Ng, S.; Moss, S. A.; Maruff, P.; Mathis, C. A.; Klunk, W. E.; Masters, C. L.; Rowe, C. C. Beta-amyloid imaging and memory in non-demented individuals: evidence for preclinical Alzheimer's disease. *Brain* **2007**, *130*, 2837−2844.
(40) Chen, K.; Cui, M. Recent progress in the development of metal complexes as beta-amyloid imaging probes in the brain. *Med. Chem. Comm.* **2017**, *8*, 1393−1407.
(41) Mehta, M.; Adem, A.; Sabbagh, M. New acetylcholinesterase inhibitors for Alzheimer's disease. *Int. J. Alzheimers Dis.* **2012**, *2012*, 728983.
(42) Barten, D. M.; Albright, C. F. Therapeutic strategies for Alzheimer's disease. *Mol. Neurobiol.* **2008**, *37*, 171−186.
(43) Hroch, L.; Aitken, L.; Benek, O.; Dolezal, M.; Kuca, K.; Gunn-Moore, F.; Musilek, K. Benzothiazoles - scaffold of interest for CNS targeted drugs. *Curr. Med. Chem.* **2015**, *22*, 730−747.
(44) Sagnou, M.; Mavroidi, B.; Shegani, A.; Paravatou-Petsotas, M.; Raptopoulou, C.; Psycharis, V.; Pirmettis, I.; Papadopoulos, M. S.; Pelecanou, M. Remarkable Brain Penetration of Cyclopentadienyl M(CO)(3)(+) (M = Tc-99m, Re) Derivatives of Benzothiazole and Benzimidazole Paves the Way for Their Application as Diagnostic, with Single-Photon-Emission Computed Tomography (SPECT), and Therapeutic Agents for Alzheimer's Disease. *J. Med. Chem.* **2019**, *62*, 2638−2650.
(45) Bolognesi, M. L.; Bartolini, M.; Tarozzi, A.; Morroni, F.; Lizzi, F.; Milelli, A.; Minarini, A.; Rosini, M.; Hrelia, P.; Andrisano, V.; Melchiorre, C. Multitargeted drugs discovery: Balancing anti-amyloid and anticholinesterase capacity in a single chemical entity. *Bioorg. Med. Chem. Lett.* **2011**, *21*, 2655−2658.
(46) Huang, L.; Su, T.; Shan, W.; Luo, Z.; Sun, Y.; He, F.; Li, X. Inhibition of cholinesterase activity and amyloid aggregation by berberine-phenyl-benzoheterocyclic and tacrine-phenyl-benzoheterocyclic hybrids. *Bioorg. Med. Chem.* **2012**, *20*, 3038−3048.
(47) Keri, R. S.; Quintanova, C.; Marques, S. M.; Esteves, A. R.; Cardoso, S. M.; Santos, M. A. Design, synthesis and neuroprotective evaluation of novel tacrine-benzothiazole hybrids as multi-targeted compounds against Alzheimer's disease. *Bioorg. Med. Chem.* **2013**, *21*, 4559−4569.
(48) Zengin, M.; Unsal-Tan, O.; Küçükkılınç, T. T.; Ayazgok, B.; Balkan, A. Design and Synthesis of 2-Substitutedphenyl Benzo[D]-Thiazole Derivatives and Their Beta-Amyloid Aggregation and Cholinesterase Inhibitory Activities. *Pharm. Chem. J.* **2019**, *53*, 322−328.
(49) Rajeshwari, R.; Chand, K.; Candeias, E.; Cardoso, S. M.; Chaves, S.; Santos, M. New Multitarget Hybrids Bearing Tacrine and Phenylbenzothiazole Motifs as Potential Drug Candidates for Alzheimer's Disease. *Molecules* **2019**, *24*, 587.
(50) Pardridge, W. M. Drug transport across the blood-brain barrier. *J. Cereb. Blood Flow Metab.* **2012**, *32*, 1959−1972.
(51) Mourtas, S.; Christodoulou, P.; Klepetsanis, P.; Gatos, D.; Barlos, K.; Antimisiaris, S. G. Preparation of Benzothiazolyl-Decorated Nanoliposomes. *Molecules* **2019**, *24*, 1540.
(52) Barrow, C. J.; Yasuda, A.; Kenny, P. T. M.; Zagorski, M. G. Solution conformations and aggregational properties of synthetic amyloid beta-peptides of Alzheimer's disease. Analysis of circular dichroism spectra. *J. Mol. Biol.* **1992**, *225*, 1075−1093.
(53) Xue, C.; Lin, T. Y.; Chang, D.; Guo, Z. Thioflavin T as an amyloid dye: fibril quantification, optimal concentration and effect on aggregation. *R. Soc. Open Sci.* **2017**, *4*, 160696.
(54) Weksler, B.; Romero, I. A.; Couraud, P. O. The hCMEC/D3 cell line as a model of the human blood brain barrier. *Fluids Barriers CNS* **2013**, *10*, 16.
(55) Markoutsa, E.; Papadia, K.; Giannou, A. D.; Spella, M.; Cagnotto, A.; Salmona, M.; Stathopoulos, G. T.; Antimisiaris, S. G. Mono and dually decorated nanoliposomes for brain targeting, in vitro and in vivo studies. *Pharm. Res.* **2014**, *31*, 1275−1289.
(56) Papadia, K.; Markoutsa, E.; Mourtas, S.; Giannou, A. D.; La Ferla, B.; Nicotra, F.; Salmona, M.; Klepetsanis, P.; Stathopoulos, G. T.; Antimisiaris, S. G. Multifunctional LUV liposomes decorated for BBB and amyloid targeting. A. In vitro proof-of-concept. *Eur. J. Pharm. Sci.* **2017**, *101*, 140−148.

https://dx.doi.org/10.1021/acs.biomac.0c00811
Biomacromolecules XXXX, XXX, XXX−XXX

(57) Stewart, J. C. M. Colorimetric determination of phospholipids with ammonium ferrothiocyanate. *Anal. Biochem.* **1980**, *104*, 10−14.
(58) Franken, L. E.; Boekema, E. J.; Stuart, M. C. A. Transmission Electron Microscopy as a Tool for the Characterization of Soft Materials: Application and Interpretation. *Adv. Sci. (Weinh)* **2017**, *4*, 1600476.
(59) Tzanopoulou, S.; Sagnou, M.; Paravatou-Petsotas, M.; Gourni, E.; Loudos, G.; Xanthopoulos, S.; Lafkas, D.; Kiaris, H.; Varvarigou, A.; Pirmettis, I. C.; Papadopoulos, M.; Pelecanou, M. Evaluation of Re and 99mTc Complexes of 2-(4'-Aminophenyl)benzothiazole as Potential Breast Cancer Radiopharmaceuticals. *J. Med. Chem.* **2010**, *53*, 4633−4641.
(60) Immordino, M. L.; Dosio, F.; Cattel, L. Stealth liposomes: review of the basic science, rationale, and clinical applications, existing and potential. *Int. J. Nanomed.* **2006**, *1*, 297−315.
(61) Garbuzenko, O.; Barenholz, Y.; Priev, A. Effect of grafted PEG on liposome size and on compressibility and packing of lipid bilayer. *Chem. Phys. Lipids* **2005**, *135*, 117−129.
(62) Putri, D. C. A.; Dwiastuti, R.; Marchaban, M.; Nugroho, A. K. Optimization of mixing temperature and sonication duration in liposome preparation. *J. Pharm. Sci. Commun.* **2017**, *14*, 79−85.
(63) Smith, M. C.; Crist, R. M.; Clogston, J. D.; McNeil, S. E. Zeta potential: a case study of cationic, anionic, and neutral liposomes. *Anal. Bioanal. Chem.* **2017**, *409*, 5779−5787.
(64) Levine, H. Thioflavine-T Interaction with Synthetic Alzheimers-Disease Beta-Amyloid Peptides - Detection of Amyloid Aggregation in Solution. *Protein Sci.* **1993**, *2*, 404−410.
(65) Haass, C.; Selkoe, D. J. Soluble protein oligomers in neurodegeneration: lessons from the Alzheimer's amyloid beta-peptide. *Nat. Rev. Mol. Cell Biol.* **2007**, *8*, 101−112.
(66) Mourtas, S.; Lazar, A. N.; Markoutsa, E.; Duyckaerts, C.; Antimisiaris, S. G. Multifunctional nanoliposomes with curcumin-lipid derivative and brain targeting functionality with potential applications for Alzheimer disease. *Eur. J. Med. Chem.* **2014**, *80*, 175−183.
(67) Taylor, M.; Moore, S.; Mourtas, S.; Niarakis, A.; Re, F.; Zona, C.; La Ferla, B.; Nicotra, F.; Masserini, M.; Antimisiaris, S. G.; Gregori, M.; Allsop, D. Effect of curcumin-associated and lipid ligand-functionalized nanoliposomes on aggregation of the Alzheimer's Abeta peptide. *Nanomedicine* **2011**, *7*, 541−550.
(68) Bana, L.; Minniti, S.; Salvati, E.; Sesana, S.; Zambelli, V.; Cagnotto, A.; Orlando, A.; Cazzaniga, E.; Zwart, R.; Scheper, W.; Masserini, M.; Re, F. Liposomes bi-functionalized with phosphatidic acid and an ApoE-derived peptide affect Abeta aggregation features and cross the blood-brain-barrier: implications for therapy of Alzheimer disease. *Nanomedicine* **2014**, *10*, 1583−1590.
(69) Xiong, N.; Zhao, Y.; Dong, X.; Zheng, J.; Sun, Y. Design of a Molecular Hybrid of Dual Peptide Inhibitors Coupled on AuNPs for Enhanced Inhibition of Amyloid beta-Protein Aggregation and Cytotoxicity. *Small* **2017**, *13*, 1601666.
(70) Zhao, G.; Dong, X.; Sun, Y. Self-Assembled Curcumin-Poly(carboxybetaine methacrylate) Conjugates: Potent Nano-Inhibitors against Amyloid beta-Protein Fibrillogenesis and Cytotoxicity. *Langmuir* **2019**, *35*, 1846−1857.
(71) Jha, A.; Ghormade, V.; Kolge, H.; Paknikar, K. M. Dual effect of chitosan-based nanoparticles on the inhibition of beta-amyloid peptide aggregation and disintegration of the preformed fibrils. *J. Mater. Chem. B* **2019**, *7*, 3362−3373.
(72) Plissonneau, M.; Pansieri, J.; Heinrich-Balard, L.; Morfin, J. F.; Stransky-Heilkron, N.; Rivory, P.; Mowat, P.; Dumoulin, M.; Cohen, R.; Allémann, É.; Tóth, É.; Saraiva, M. J.; Louis, C.; Tillement, O.; Forge, V.; Lux, F.; Marquette, C. Gd-nanoparticles functionalization with specific peptides for beta-amyloid plaques targeting. *J. Nanobiotechnol.* **2016**, *14*, 60.
(73) Markoutsa, E.; Papadia, K.; Clemente, C.; Flores, O.; Antimisiaris, S. G. Anti-Aβ-MAb and dually decorated nanoliposomes: effect of Aβ1-42 peptides on interaction with hCMEC/D3 cells. *Eur. J. Pharm. Biopharm.* **2012**, *81*, 49−56.
(74) Papadia, K.; Markoutsa, E.; Antimisiaris, S. G. How do the physicochemical properties of nanoliposomes affect their interactions with the hCMEC/D3 cellular model of the BBB? *Int. J. Pharm.* **2016**, *509*, 431−438.

https://dx.doi.org/10.1021/acs.biomac.0c00811
Biomacromolecules XXXX, XXX, XXX−XXX